

4. CHEMISTRY OF THE LOWER SHEETED DIKE COMPLEX, HOLE 504B (LEG 148): INFLUENCE OF MAGMATIC DIFFERENTIATION AND HYDROTHERMAL ALTERATION¹

Wolfgang Bach,^{2,3} Jörg Erzinger,² Jeffrey C. Alt,⁴ and Damon A.H. Teagle⁴

ABSTRACT

We present major- and trace-element data on the lower sheeted dike complex (SDC) drilled during ODP Leg 148 in Hole 504B. Similar to previously studied rocks from the upper sections of Hole 504B, the rocks recovered during Leg 148 are mildly to moderately evolved mid-ocean ridge basalts (MORB) ranging in their MgO concentrations from 7.8 to 10.0 wt%. The rocks exhibit the same sort of depletion as the lavas of Hole 504B, characterized by very low incompatible element abundances (e.g., TiO₂ = 0.54–1.03 wt%, Zr = 29–53 ppm, and Ce = 2.2–5.5 ppm). Chondrite-normalized La/Sm and Nb/Zr ratios are markedly lower than average N-MORB, suggesting a highly depleted mantle source. Fractional crystallization of plagioclase, olivine, ± clinopyroxene can account for most of the chemical variability, whereby the degree of fractionation is less than 50%. The chemical effects of alteration are more difficult to distinguish because they can sometimes have the same consequences as magmatic differentiation. Formation of chlorite, amphibole, albite-oligoclase, and titanite replacing groundmass and primary minerals are typical for all samples. The results of this type of alteration are slight increases of MgO and H₂O and decreases of CaO and SiO₂. TiO₂, MnO, Zr, and the REEs appear to slightly decrease with increasing extents of alteration. Halos and patches of intensive alteration are common in the lower SDC. The alteration halos show perplexing chemical trends with no clear relationship to the degree of alteration. The alteration patches are significantly enriched in H₂O and highly depleted in Cu (Zn) and S. This makes the patches in the lower SDC possible sources for base-metal deposits in the oceanic crust. The patches are also significantly depleted in REE, Zr, Nb, Ti, and exhibit positive Eu anomalies. Theoretical considerations and mass-balance calculations indicate that this behavior is probably not only the consequence of intensive alteration but requires primary chemical differences between the patches and the neighboring diabases. It remains unclear how far such differences could be related to magmatic differentiation processes within the dikes. The puzzling question of the nature of these alteration patches deserves further attention.

INTRODUCTION

Ocean Drilling Program (ODP) Leg 148 was the seventh return to Hole 504B and deepened the drill hole to a final depth of 2111 m below seafloor (mbsf). Hole 504B is the deepest drill hole in the oceanic crust and serves as a reference for the structure and petrology of oceanic crustal Layers 2. Hole 504B drilling and research history comprises 15 years of intense technical and scientific effort during which indispensable information on the petrology, chemistry and physics of the upper oceanic crust has been collected. Previous studies have shown that the upper extrusive section consists of chemically different types of basalts comprising highly depleted basalts, typical mid-ocean ridge basalts (N-MORB), and enriched basalts (E-MORB) (e.g., Tual et al., 1985), thus displaying a time record of the temporal variability of the mantle source. Studies of secondary minerals resulted in the reconstruction of a complex multi-stage alteration history in the volcanic section and the sheeted dikes including ore-forming processes in a transition zone (e.g., Alt et al., 1986).

Other points of great interest are the physical properties of the oceanic crust. The provocative finding of Legs 140 and 148 has been that seismic wave velocities steadily increase downward and reach values thought to be typical for oceanic Layer 3 (Dick, Erzinger, Stokking, et al., 1992; Alt, Kinoshita, Stokking, et al., 1993). However, the rocks of the last section drilled during Leg 148 are still dia-

bases of the sheeted dike complex. This finding has stimulated a new discussion on the nature of the seismic Layer 2/3 boundary and has given rise to the question of whether the seismic Layer 2/3 boundary is an alteration front rather than the dike/gabbro transition (Detrick et al., 1994).

The current depth of Hole 504B appears to be representative of the lowermost part of the sheeted dike complex. Evidence for this presumption arises from the observation that base-metal depletions thought to be typical of root zones of hydrothermal vent fluids have been detected in the lower part of the hole (Alt et al., 1995; Zuleger et al., 1995). Such root zones have been found to occur in ophiolites just above the magma reservoir (Richardson et al., 1987; Harper et al., 1988; Schiffman et al., 1990; Nehlig et al., 1994).

In this paper we report major and trace-element data for 30 rocks from the lowermost 110.6 m of the sheeted dike complex. The study is a continuation of the work by Zuleger et al. (1995) and follows the same sampling and analyzing strategy, making our data directly comparable to the Zuleger et al. (1995) data set. Most of the samples were also studied for their stable isotope composition and secondary mineral chemistry and the results are given by Alt et al. (this volume). We placed emphasis on the variability of chemical compositions in diabases altered to various extents. Our results indicate increasing mobility of nominally immobile elements with increasing degree of alteration, resulting in incompatible element depletions of highly altered rocks. In contrast, changes in major-element compositions are less obvious. Possible primary and secondary mechanisms causing these depletions are discussed below.

GEOLOGICAL SETTING AND PREVIOUS STUDIES

Hole 504B is located in 5.9 Ma crust, about 200 km south of the Costa Rica Rift Zone in the Eastern Pacific ocean (1°13.611'N, 83°43.818'W; see Fig. 1). The Costa Rica Rift Zone is an east-west-

¹Alt, J.C., Kinoshita, H., Stokking, L.B., and Michael, P.J. (Eds.), 1996. *Proc. ODP, Sci. Results*, 148: College Station, TX (Ocean Drilling Program).

²GeoForschungsZentrum Potsdam, Projektbereich 4.2, Telegrafenberg A50, D-14473 Potsdam, Federal Republic of Germany. Bach: wbach@gfz-potsdam.de; Erzinger: erz@gfz-potsdam.de

³Present address: Universität Potsdam, Institut für Geowissenschaften, Postfach 601553, D-14415 Potsdam, Federal Republic of Germany.

⁴Department of Geological Sciences, 2534 C.C. Little Building, The University of Michigan, Ann Arbor, MI 48109-1063, U.S.A. Alt: jalt@umich.edu; Teagle: teagle@umich.edu

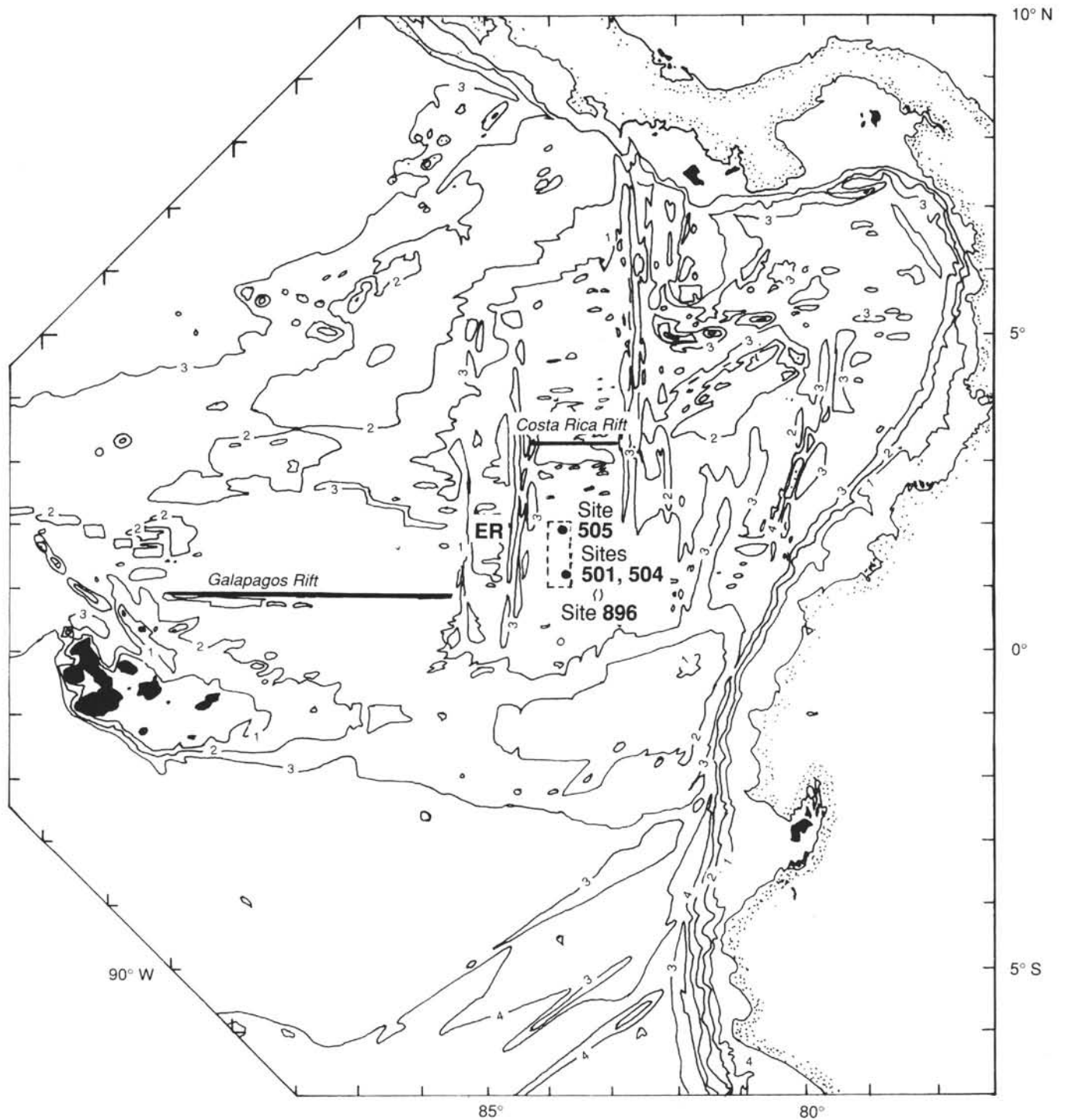


Figure 1. Location of DSDP Sites 501 and 505, DSDP/ODP Site 504, and ODP Site 896 south of the Costa Rica Rift in the eastern equatorial Pacific (after Hobart et al., 1985).

trending intermediate spreading center with a southward spreading rate of 36 mm/yr (Hey et al., 1977).

Several previous studies have shown that the basaltic rocks from Hole 504B are olivine- and plagioclase- (\pm clinopyroxene-) bearing tholeiites, representing moderately evolved MORB (Autio and Rhodes, 1983; Etoubleau et al., 1983; Hubberten et al., 1983; Marsh et al., 1983; Emmermann, 1985; Kempton et al., 1985; Tual et al., 1985; Autio et al., 1989; Sparks et al., 1995; Zuleger et al., 1995). In terms of their trace-element compositions most rocks (>98%) are highly depleted in incompatible elements (Na, Ti, Zr, Y, REE, Ta,

Nb, etc.) when compared to average N-MORBs. In addition to this dominant type of depleted composition are four other types of basalts (Kempton et al., 1985) that display either higher degrees of magmatic differentiation (Kempton et al.'s type M') or variations in their trace-element characteristics (Kempton et al.'s types M, T, and E). Using a more common terminology, one can say that less than 2% of the rocks are not highly depleted and range in composition from typical N-MORB to T-MORB and E-MORB. The numerous investigators of the igneous petrology and geochemistry of Hole 504B rocks agree overall in attributing these differences to mantle heterogeneities and/

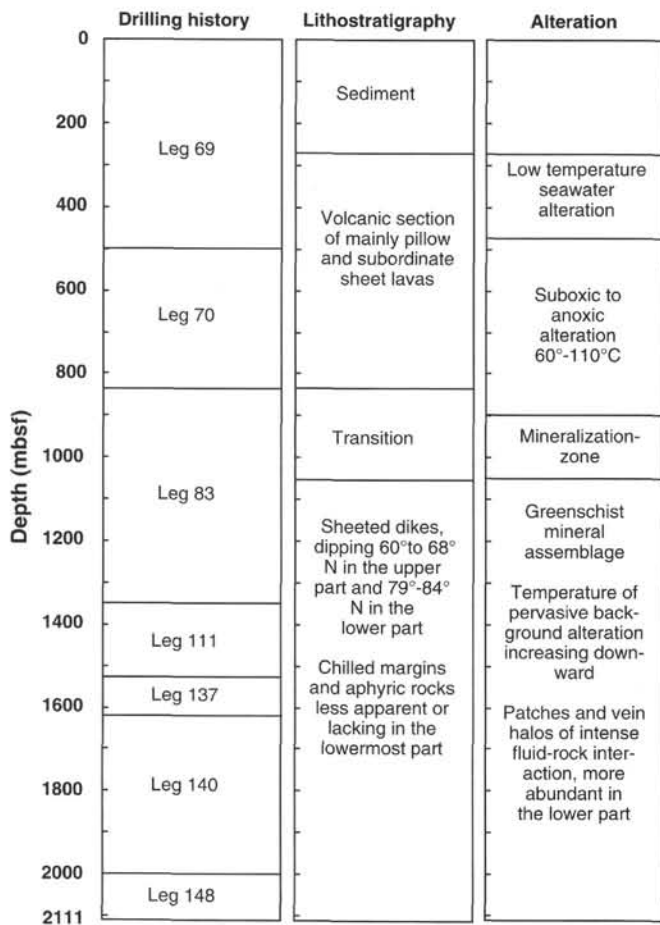


Figure 2. Summary of the site drilling history, and the lithostratigraphy and alteration of Hole 504B rocks.

or to multi-stage melting processes, with the depleted basalts representing a mantle that was depleted as a result of earlier melting processes.

Isotopic studies support the idea of a heterogeneous mantle (e.g., Barrett, 1983; Kusakabe et al., 1989; Shimizu et al., 1989). Another peculiarity of the Hole 504B basalts is their high Ca/Na ratio and the corresponding calcic plagioclase compositions (up to An_{94} , Natland et al., 1983). Liquidus temperatures calculated from glass compositions vary in a narrow range possibly indicating a nearly steady-state magmatic system (Natland et al., 1983).

Figure 2 summarizes the drilling history, structural units, and alteration types observed in Hole 504B. Alteration style changes in the extrusive series from oxidative to non-oxidative and this correlates with changes in chemical compositions (e.g., a drastic decrease in the concentrations of alkaline elements; Hubberten et al., 1983; Alt et al., 1986). Leg 83 drilled a transition zone of extrusive flows cross-cut by numerous dikes (Alt and Emmermann, 1985). The upper part of this transition zone, the so-called stockwork mineralization zone, is characterized by profound impregnations with sulfides resulting in increased Zn, Cu, Fe, and S concentrations (Alt and Emmermann, 1985; Alt et al., 1986). The stockwork ores are thought to be precipitated when hot upwelling metal-bearing hydrothermal fluids mixed with cold downwelling seawater at a prominent permeability boundary between the more permeable extrusives and the less permeable sheeted dikes (Alt et al., 1986).

Studies of secondary mineral chemistry and paragenesis made a detailed reconstruction of the post-magmatic history of the upper crust in Hole 504B possible. Alt et al. (1995) and Laverne et al.

(1995) proposed five alteration stages in the lower sheeted dike section beginning with circulation of high-temperature fluids (500°–600°C) along fluid conduits of high permeability and formation of secondary clinopyroxene and calcic plagioclase in veins, halos, and patches of strong alteration. The second stage was pervasive circulation of up to 400°C hydrothermal fluids and deposition of actinolitic hornblende, titanite and oligoclase, followed by amphibole, chlorite, and albite at lower temperatures. This episode was followed by upwelling of reacted fluids (Mg-depleted) at temperatures of about 320°C and precipitation of epidote and quartz in crosscutting veins and fill in pore space. During the fourth stage, anhydrite formation occurred locally as a result of recharge of seawater into the hot crust. Finally, highly evolved hydrothermal fluids at lower temperatures (<250°C) circulated through the off-axis crust and led to the formation of laumontite and prehnite.

The sheeted dikes below the transition zone have been altered under greenschist facies conditions with temperatures increasing downward (Alt et al., 1989; Alt et al., 1995; Laverne et al., 1995). An interesting feature of the lower sheeted dike complex is the presence of highly altered zones along amphibole veins (halos) and irregularly formed patches of strong alteration. The latter show drastically lower abundances of incompatible and nominally immobile elements (Ti, Zr, Y, REE, etc.) (Zuleger et al., 1995; Sparks, 1995). It is yet unclear to what extent these chemical depletions are of primary origin as opposed to alteration processes.

SAMPLE PREPARATION AND ANALYTICAL PROCEDURES

Rock powders for all chemical analyses and chips for all thin sections were prepared from the same piece of rock. After culling rock chips for thin sections from the remaining material, areas with large phenocrysts were cut off. The samples were then rinsed with distilled water, crushed in a steel mortar, and powdered in an agate mill.

Major-element oxides were analyzed by X-ray fluorescence (XRF) on samples prepared as fused disks of lithium metaborate (sample-to-flux ratio 1:4). A Philips PW 1400 computerized spectrometer was used and a Philips "alphas program" calculated the concentrations. Ferrous iron was determined by manganometric titration, and H_2O^+ by a LECO analyzer RC-412. Sulfur analyses were performed using a LECO sulfur determinator CS 225.

Determinations of Cr, Ni, Cu, Zn, Ga, Sr, Y, and Zr were conducted by XRF on pressed powder pellets. The rhodium Compton peak of the X-ray tube was used for matrix corrections. International reference rocks were used for calibration of the XRF method.

The rare-earth elements (REE) Li, Rb, Sc, Nb, Th, and U were determined by mass spectrometry with an inductively coupled plasma as ionization source (ICP-MS, VG Plasmaquad PQ 2+). We used a sample preparation and a modified ICP-MS technique originally described by Garbe-Schönberg (1993). A detailed description of our modified method is given by Zuleger et al. (this volume). Cr, Ni, Cu, Zn, Ga, Sr, Y, and Zr were also determined by ICP-MS. Except Zr, and to a lesser extent Y, all ICP-MS data are comparable to the respective XRF values (see Zuleger et al., this volume, for a comparison of XRF and ICP-MS data).

Previous studies of Hole 504B rocks revealed that chemical data sets of various laboratories differ significantly because of different analytical accuracies and precisions (Dick, Erzinger, Stokking, et al., 1992, and Boström and Bach, 1995, for a discussion). We therefore carefully tested our data with the reference data from Govindaraju (1994) and with data from other laboratories to ensure proper analytical accuracy.

Table 1 presents the analytical accuracy and precision of the XRF data. Assuming the analytical error is close to twice the standard deviation, the precision for the major elements is better than 1.5 rel% and the precision for the trace elements is better than 10 rel%, mostly better than 5 rel%.

Table 1. Precision and accuracy of XRF data.

	Rec. value DR-N	Mean (N = 7)	1 σ	Relative SD (%)
Major elements (wt%):				
SiO ₂	52.85	53.25	0.10	0.18
TiO ₂	1.09	1.08	0.01	0.70
Al ₂ O ₃	17.52	17.87	0.04	0.25
Fe ₂ O ₃	9.70	9.68	0.02	0.23
MnO	0.22	0.22	0.00	0.00
MgO	4.40	4.42	0.02	0.50
CaO	7.05	7.07	0.02	0.24
Na ₂ O	2.99	3.08	0.01	0.44
K ₂ O	1.70	1.72	0.004	0.22
P ₂ O ₅	0.25	0.24	0.00	0.00
	Rec. value BHVO-1	Mean (N = 9)	1 σ	Relative SD (%)
Trace elements (ppm):				
Cr	289	297	5.6	1.9
Ni	121	114	1.7	1.5
Cu	136	142	2.4	1.7
Zn	105	103	1.1	1.1
Ga	21	21.0	0.9	4.4
Rb	11	10.6	0.7	7.0
Sr	403	398	2.4	0.60
Y	27.6	26.2	1.4	5.3
Zr	179	172	3.2	1.9
Nb	19	18.8	0.4	2.4

Notes: The recommended (Rec.) values are from Govindaraju (1989). The international standard rocks DR-N and BHVO-1 were used for major elements and trace elements, respectively. SD = standard deviation.

Table 2 compares our analyses of the international reference rock BIR-1 with three other laboratories using similar methods and instruments. The precision of our data is usually better than 10 rel%. A comparison between our "BAS 140" XRF and ICP-MS data and the "BAS 140" data of Sparks (1995), Zuleger et al. (1995) and Zuleger et al. (this volume) is given in Table 3. The results of all elements are in very good agreement, indicating that a direct comparison of our data with the data set of Sparks (1995) and Zuleger et al. (1995, this volume) is allowed.

Chemical compositions of the samples under investigation are given in Table 4. Cs was measured using ICP-MS, but the concentrations are below the detection limit of 20 ppb. Ba and Pb ICP-MS data have been found to be affected by solvent blanks and memory problems at the low concentration level of Hole 504B rocks, and hence are not reported. XRF data of Zr correlate excellently with ICP-MS Nb, REE, and Th data, whereas ICP-MS data of Zr do not. Zr ICP-MS values are systematically lower than Zr XRF values, possibly because of incomplete dissolution of trace minerals. Because Hf does correlate only with the (poor) Zr ICP-MS data but does not correlate with any other element, we assume that both Zr and Hf ICP-MS data are poor and thus they are not reported. Interestingly, we did not have these problems with the Leg 148 Hole 896A rocks (Teagle et al., this volume), suggesting that indeed it may be a problem of incomplete dissolution of trace minerals (zircon?) that occur in the lower sheeted dikes but not in the lavas.

RESULTS

Petrography

All samples are sparsely to moderately phryic diabases with plagioclase, olivine, clinopyroxene, and rare spinel phenocrysts. Grain-size analyses and the distribution of chilled margins led Umino (1995) to develop a model of multiple dike intrusions with up to 8.5-m-thick dike packets. Grain size data display decreasing grain sizes from 2000 to 2042 mbsf, followed by overall increases in average grain-sizes downwards (Alt, Kinoshita, Stokking, et al., 1993).

Table 2. Comparison of trace-element data obtained by ICP-MS with certified values of the international reference rock BIR-1 and data from three other laboratories.

	BIR-1 reference	This work (Mean)	1 σ	Univ. Kiel ICP-MS	MPI Mainz SSMS	Univ St. John's ICP-MS
Li	3.4	3.36	0.32			3.1
Sc	44	41.3	1.4	41.9		43
Cr	382	380	36	343		
Co	51.4	53	4	52.4		
Ni	166	161	14	162		
Cu	126	117	5	120		
Zn	71	73	4			
Ga	16	15	0.9			
Rb	0.25	0.27	0.08	0.2	0.272	0.23
Sr	108	110	7	93.7	109	111
Y	16	13.2	0.8	15	16.8	15.6
Zr	15.5	13.4	0.9	12.7	12.1	16.3
Nb	0.6	0.49	0.04	0.49	0.49	0.59
La	0.62	0.67	0.07	0.54	0.594	0.6
Ce	1.95	1.91	0.06	1.74	1.83	1.87
Pr	0.38	0.4	0.04	0.33	0.341	0.36
Nd	2.5	2.4	0.09	2.13	2.19	2.3
Sm	1.1	1.08	0.11	1	1.07	1.06
Eu	0.54	0.56	0.05	0.47	0.457	0.56
Gd	1.85	1.73	0.08	1.53	1.52	1.73
Tb	0.36	0.37	0.03	0.31	0.3	0.36
Dy	2.5	2.6	0.15	2.23	2.26	2.69
Ho	0.57	0.58	0.05	0.51	0.55	0.61
Er	1.7	1.66	0.04	1.49	1.5	1.7
Tm	0.26	0.25	0.02	0.22	0.23	0.24
Yb	1.65	1.66	0.09	1.51	1.36	1.63
Lu	0.26	0.25	0.02	0.22	0.23	0.25
Hf	0.6	0.61	0.04	0.57	0.36	0.60
Th	0.03	0.037	0.002	0.024	0.031	0.036

Notes: BIR-1 data from Govindaraju (1994). University (Univ.) of Kiel data from Garbe-Schönberg (1993). Max-Planck-Institut (MPI) Mainz data from Jochum et al. (1990). University of Saint John's data from Jenner et al. (1990). ICP-MS = inductively coupled plasma-mass spectrometry, SSMS = spark-source mass spectrometry. Concentrations are in parts per million (ppm).

The rocks are hydrothermally altered to various extents. To quantify the extent of alteration we visually estimated the percentage of secondary minerals, which we refer to below as "degree of alteration." During Leg 148, thin sections were point-counted for alteration minerals. The deviation of our visual estimates from the shipboard point counts is less than 10%. The Shipboard Scientific Parties of Legs 137, 140, and 148 (Becker, Foss, et al., 1992; Dick, Erzinger, Stokking, et al., 1992; Alt, Kinoshita, Stokking, et al., 1993) identified at least three different types of alteration. A frequency distribution of the degree of alteration in the different rock types is shown in Figure 3. *First*, dark gray diabases affected by pervasive background alteration up to 60%, but usually between 10% and 40%. The diabases are affected by a pervasive background alteration during which olivine was completely replaced by various secondary minerals, clinopyroxene was partly replaced mostly by amphibole, and plagioclase remained virtually unaltered except albitization along cracks. *Second*, alteration halos along amphibole veins show discoloration and variable degrees of alteration (Fig. 3) but are usually more extensively recrystallized than the host rock. The most obvious difference between the halos and the adjacent host rock is the higher abundance of amphibole in the halos (35%–70%) as compared to the host diabase (5%–35%). This amphibole replaces virtually all magmatic clinopyroxene in the halos. Generally, veins and halos are more abundant in the section drilled during Leg 148 (21 veins/m, 1.2 vol% veins) as compared to Leg 140 (15 veins/m, 0.6 vol% veins) (Alt, Kinoshita, Stokking, et al., 1993). *Third*, patches of intense alteration up to 80% recrystallized vary from centimeter to decimeter scale and occur as irregular to subrounded, dark green areas grading into host diabase. Within the patches, 45%–80% of the igneous minerals are replaced by secondary phases, typically amphibole (ranging in composition from actinolite to actinolitic hornblende to magnesiohornblende), chlorite, secondary magnetite, and titanite. The halos

Table 3. Comparison of chemical data of the laboratory standard BAS 140.

	Sparks (1995)	Zuleger et al. (1995)	This study (Mean)	1 σ
Major elements (wt%):				
SiO ₂	50.6	50.6	50.4	0.05
TiO ₂	0.99	1.00	0.99	0.004
Al ₂ O ₃	14.58	14.6	14.6	0.02
Fe ₂ O ₃	11.08	11.3	11.2	0.03
MnO	0.19	0.19	0.18	0.004
MgO	8.14	8.21	8.15	0.04
CaO	12.41	12.5	12.5	0.03
Na ₂ O	1.85	1.78	1.78	0.01
K ₂ O	ND	ND	ND	
P ₂ O ₅	0.065	0.08	0.076	0.005
Trace elements (ppm):				
Cr	192	194	192	1.7
Ni	85	81	81	0.5
Cu	84	83	82	1
Zn	85	78	78	0.5
Ga	15.6	16	16	0.6
Sr	45.5	47	47	0.6
Y	26.6	27	30	0.9
Zr	44.8	49	49	0.6
	Sparks (1995)	Zuleger et al. (this volume)	This study (Mean)	1 σ
Li	ND	1.1	1.11	0.07
Sc	ND	43	44	1
Nb	ND	0.56	0.55	0.02
La	ND	1.0	0.98	0.07
Ce	ND	3.8	3.8	0.1
Pr	ND	0.78	0.76	0.05
Nd	ND	4.9	4.8	0.1
Sm	ND	2.08	2.06	0.05
Eu	ND	0.8	0.82	0.05
Gd	ND	3.2	3.1	0.1
Tb	ND	0.60	0.62	0.04
Dy	ND	4.5	4.4	0.15
Ho	ND	0.98	0.96	0.02
Er	ND	3.0	2.9	0.1
Tm	ND	0.44	0.43	0.02
Yb	ND	2.9	2.85	0.04
Lu	ND	0.45	0.42	0.02
Hf	ND	1.24	1.12	0.04
Th	ND	ND	0.021	0.006
U	ND	ND	0.007	0.003

Note: ND = not determined. Rare-earth elements in parts per million (ppm).

and the patches are thought to represent areas of extensive fluid-rock interaction. Only one sample (Section 148-504B-247R-1, Piece 10) shows both patches and haloed veins, where the age relationship appears to be such that the patch was formed before the vein (Alt, Kinoshita, Stokking et al., 1993). Alt et al. (1985, 1989, 1995) reported millimeter-scale amygdules that apparently represent primary vugs or pore space filled by amphibole, chlorite, laumontite, and epidote in the alteration patches. These vugs can make up 15% to 20% of the rock volume. Such amygdules were observed in one sample from Leg 148 (Section 148-504B-252R-1, Piece 5) and consist of needle-like amphibole. Thus, high primary porosity was present at least locally in the Leg 148 section. Patches appear to be generally restricted to regions with large average grain sizes (i.e., the center parts of dike packets). Rock type and alteration type of all samples under investigation are given in the heading of Table 4. It is important to note that many samples are composed of different types of alteration (e.g., dark + patch), this information is also given in Table 4. The classification into groups (D = dark diabase, H = Halo, and P = patch) was made on the basis of the prevailing type of alteration (for a more complete petrographic documentation and photomicrographs of the three rock types, see Alt, Kinoshita, Stokking, et al. 1993; Alt et al., this volume; and Vanko et al., this volume). The Leg 140 Shipboard Scientific Party (Dick, Erzinger, Stokking, et al., 1992) observed a fourth rock type of light gray color and more intense background alteration as compared to the dark diabases. This type of rock was not sampled during Leg 148.

Chemical Composition

Rocks from the sheeted dike complex (SDC) display an overall remarkable homogeneity in chemical compositions. The compositional range (in wt%) of samples from Leg 148 is as follows: SiO₂ = 47.9–50.3, TiO₂ = 0.54–1.03, Al₂O₃ = 14.8–17.3, FeO* = 7.5–9.7, MgO = 7.8–10, CaO = 12.3–14.0, and Na₂O = 1.57–2.11. These ranges are similar to those previously reported for the diabases of Hole 504B (Autio et al., 1989; Zuleger et al., 1995; Sparks, 1995). Basaltic rocks from Hole 504B have been classified as olivine to quartz normative tholeiites of relatively primitive composition (Hubberten et al., 1983; Emmermann, 1985). Trace-element compositions (in ppm) of Leg 148 rocks are also similar to those from previous legs: Cr = 266–399, Ni = 86–167, Zr = 29–53, Y = 16–27, Sr = 50–66, La = 0.54–1.53, Ce = 2.2–5.5, Sm = 1.1–2.3, and Yb = 1.7–2.5. Overall, the diabases display the trace-element characteristics of highly depleted and relatively primitive basalts. Evidence for the unusual depletion of the mantle source arises from the low (La/Sm)_N (0.29–0.42) and high Zr/Nb (83–140) ratios. The values differ drastically from average depleted mid-ocean ridge basalts ([La/Sm]_N = 0.65, and Zr/Nb = 32; Hofmann, 1988). The generally low concentrations of incompatible elements and the high MgO, Cr, and Ni values indicate that basaltic melts must have been primitive to mildly evolved. Th/U ratios of the lower oceanic crust have been rarely reported so far but they are important to construct mantle evolution models. Our data reveal Th/U ratios of the lower SDC in Hole 504B of 3 ± 0.5. This is not significantly different from the average Th/U of fresh MORBs (2.6; Hofmann, 1988).

All rocks of the SDC are hydrothermally altered to various extents accompanied with chemical changes as a result of varying mobilities of elements during recrystallization. On the other hand, basalt glasses from the volcanic section (Natland et al., 1983) show significant chemical variability, probably because of magmatic differentiation occurring upon cooling of a magma reservoir.

DISCUSSION

Chemical Variation With Depth

The chemical variation of the lower SDC rocks including samples from Leg 140 (Zuleger et al., (1995) and Leg 148 (this work) are shown in Figure 4. Depth intervals with abundant patches are marked by the shaded areas.

Generally, the degree of alteration ranges to higher values in the sections with alteration patches. TiO₂, MnO, Zr, and CaO show lowest and water shows highest concentrations in these zones of high alteration. Two sections have MgO and Ni contents higher than usual, one from 1700 to 1730 mbsf, and a second one at the lowermost part of the drill hole (2080–2111 mbsf). In these intervals, MgO values are between 9 and 10 wt% and Ni varies from 125 to 190 ppm. Some elements display a crude sawtooth-like pattern in their variation with depth. This is most clearly seen in the TiO₂, Zr, and MnO data and the reflected type of pattern is delineated by Ni and, less obvious, MgO. This type of pattern becomes less apparent in depth intervals where the sample spacing is wide (e.g., 1830–1900 mbsf). In the depth interval 2000–2111 mbsf drilled during Leg 148 are trends of decreasing MgO and Ni and increasing TiO₂, Zr, and SiO₂ from 2000 to about 2050 mbsf, followed by reversed trends from 2050 to the bottom of the hole. The water contents and degrees of alteration exhibit a similar trend of decreasing values down to 2050 mbsf and increasing values below. Zuleger et al. (1995) discussed a possible relationship between such vertical variations and the intrusion of dike packets with varying compositions. The new data support this possibility as the systematic trends in Ni and Zr, for example, are well developed in the lower section and these trends correlate with systematic decreases and increases in the average grain sizes (Alt, Kinoshita, Stokking, et al. 1993). Because the dikes are steeply dipping

Table 4. Chemical compositions of Hole 504B diabases.

Core, section: Interval (cm): Piece no.: Depth (mbsf): Lith. unit: Rock type: Alteration type:	239R-1 45-51 14-HALO 2000.85 271 M-POD Halo	240R-1 41-45 11 2007.31 273 S-PPD Dark patch P 45	240R-1 95-99 22 2007.85 274 M-OPCD Patch + vugs P 70	241R-1 11-15 4 2016.61 276 M-POCD Dark (+ patch?) D 30	241R-1 42-46 9 2016.92 276 M-POCD Dark act.veins D 30	241R-1 95-98 19 2017.45 276 M-POCD Halo + amph. veins H 65	241R-1 117-118 20 2017.67 276 M-POCD Patch P 70	242R-1 0-5 1 2025.90 276 M-POCD Patch + vugs + dark P 60	245R-1 48-51 16 2043.28 281 S-PPD Dark D 50	246R-1 8-11 4 2052.28 283 S-POD Halo + amph. veins + dark H 30
Major elements (wt%):										
SiO ₂	48.6	48.9	48.9	49.3	47.9	48.7	48.2	49.0	49.7	48.7
TiO ₂	0.87	0.63	0.65	0.80	0.79	0.76	0.67	0.71	0.90	0.83
Al ₂ O ₃	16.5	17.3	16.6	17.1	16.8	16.4	17.3	16.2	15.6	16.0
FeO	6.47	6.25	6.67	6.07	5.95	5.96	6.20	6.51	6.62	6.71
Fe ₂ O ₃	1.74	1.77	2.06	1.59	1.88	2.03	1.76	2.44	2.19	2.46
MnO	0.13	0.13	0.13	0.14	0.13	0.14	0.13	0.14	0.13	0.16
MgO	7.82	8.79	8.47	8.47	8.73	8.47	8.52	9.32	8.24	9.13
CaO	12.9	13.0	12.5	14.0	13.7	13.5	13.0	12.8	13.1	12.7
Na ₂ O	2.11	1.88	1.91	1.89	1.80	1.82	1.90	1.83	2.03	1.79
K ₂ O	<0.01	0.01	0.01	<0.01	<0.01	<0.01	0.01	0.01	0.01	<0.01
P ₂ O ₅	0.06	0.04	0.04	0.05	0.06	0.05	0.04	0.05	0.06	0.06
H ₂ O	1.76	1.65	1.76	1.32	1.55	1.59	1.62	1.72	1.13	1.34
CO ₂	0.25		0.11		0.07	0.1		0.09	0.1	0.08
Sum	99.2	100.4	99.8	100.8	99.3	99.6	99.3	100.8	99.7	100.1
Mg#	65.8	68.9	66.3	69.1	69.3	68.3	68.4	68.0	65.5	67.0
FeO*	8.04	7.84	8.53	7.50	7.64	7.78	7.78	8.70	8.59	8.93
Fe ³⁺ /ΣFe	0.20	0.20	0.22	0.19	0.22	0.23	0.20	0.25	0.23	0.25
Trace elements (ppm):										
S		<20	<20	30	70	<20	<20	35	80	310
Cr		371	370	339	334	330	383	345	266	311
Ni		135	126	125	134	126	135	145	96	137
Cu		8	8	14	15	8	8	30	32	91
Zn		44	44	45	36	40	41	41	33	48
Ga		15	14	15	15	15	13	13	16	16
Sr		58	58	57	56	55	59	53	57	55
Y		17	20	21	26	23	16	23	27	26
Zr		31	35	40	43	39	32	37	47	43
Li		0.88		1.17			0.78			
Sc		39		41			41			
Rb		0.11		0.09			0.10			
Nb		0.27		0.31			0.26			
La		0.71		0.94			0.70			
Ce		2.72		3.49			2.62			
Nd		3.32		4.28			3.17			
Sm		1.45		1.85			1.47			
Eu		0.65		0.71			0.60			
Gd		2.15		2.61			2.05			
Tb		0.40		0.50			0.39			
Dy		3.01		3.81			2.94			
Ho		0.61		0.75			0.58			
Er		1.86		2.31			1.84			
Tm		0.27		0.33			0.26			
Yb		1.84		2.22			1.81			
Lu		0.28		0.32			0.26			
Th		0.016		0.017			0.015			
U		0.006		0.006			0.005			
Th/U		2.88		2.91			2.95			
Zr/Nb		116		131			123			
La/Nb		2.63		3.03			2.71			
Th/Nb		0.060		0.053			0.058			
(La/Sm) _N		0.32		0.33			0.31			
(Sm/Yb) _N		0.88		0.92			0.90			

(79°–84°), it is possible that a small number of dike packets was penetrated during Leg 148, although the thickness of such packets was estimated to be less than 8.5 m (Umino, 1995). Another possibility is to assume that alteration caused the compositional trends in such a way that chlorite formation increases MgO (Ni?) and H₂O, decreases SiO₂, and the larger amounts of secondary minerals dilute incompatible elements like Ti and Zr. This dilemma makes a close inspection of the possible chemical effects of magmatic differentiation and hydrothermal alteration necessary.

Magmatic Differentiation

The effects of fractional crystallization of plagioclase and olivine (± clinopyroxene) on major-element compositions are well constrained (e.g., Bryan et al., 1976). We used crystallization models of Nielsen (1990) and Weaver and Langmuir (1990) to assess the chem-

ical effects of fractional crystallization in rocks from Hole 504B. A detailed discussion of the modeling is beyond the scope of this paper. We thus present a summary of the modeling results and their implications.

1. Crystallization of primitive Hole 504B basalts starts either with olivine or plagioclase, depending on the initial composition. Because of the generally high Ca/Na ratios of the basalts, in many cases plagioclase is the first liquidus phase and the plagioclase compositions are unusually calcic (An₈₈₋₉₄; Natland et al., 1983).

2. The first liquidus phase is joined by the second within the first 4 wt% of crystallization, after which olivine and plagioclase crystallize in a cotectic proportion of 2:1.

3. Clinopyroxene joins the fractionating mineral assemblage after 15%–30% of the initial melt is crystallized. Spinel is also an early liquidus phase and crystallizes mostly along with plagioclase.

Table 4 (continued).

Core, section:	246R-1	246R-1	246R-1	246R-1	247R-1	247R-1	247R-1	247R-1	248R-1	249R-1
Interval (cm):	26-30	46-50	66-70	103-107	18-26	30-33	46-50	76-79	55-58	4-8
Piece no.:	9	14	19	30	6	8	12	18	16	2
Depth (mbsf):	2052.46	2052.66	2052.86	2053.88	2056.88	2057.00	2057.16	2057.46	2062.35	2071.24
Lith. unit:	283	283	283	284	285	285	285	286	288	290
Rock type:	S-POD	S-POD	S-POD	S-POD	M-POD	M-POD	M-POD	M-OPD	M-CPD	M-POD
Alteration type:	Dark+ patch	Dark	Dark	Dark+ patch	Dark	Dark	Halo + amph. vein +dark	Dark	Halo	Dark
Group:	P	D	D	P	D	D	H	D	H	D
Alteration (%):	40	20	20	45	20	35	60	ND	ND	30
Major elements (wt%):										
SiO ₂	49.4	50.1	48.9	48.8	48.7	48.4	49.3	49.7	49.2	49.6
TiO ₂	0.87	0.88	0.86	0.73	0.82	0.76	0.77	0.95	0.92	1.03
Al ₂ O ₃	15.5	15.8	15.2	16.0	15.4	16.0	15.8	15.2	15.1	14.8
FeO	6.49	6.94	6.65	6.58	6.60	6.03	6.66	7.26	6.79	7.34
Fe ₂ O ₃	2.78	2.66	2.86	2.11	2.97	2.78	1.85	2.16	2.44	2.59
MnO	0.16	0.17	0.17	0.15	0.16	0.15	0.14	0.17	0.16	0.19
MgO	8.86	8.90	8.70	9.13	9.14	9.15	9.05	8.37	8.62	8.37
CaO	12.9	12.9	12.9	13.0	12.8	13.2	13.1	12.9	13.0	13.0
Na ₂ O	1.85	1.87	1.83	1.74	1.76	1.71	1.82	1.91	1.87	2.11
K ₂ O	<0.01	<0.01	<0.01	<0.01	<0.01	<0.01	0.01	<0.01	<0.01	<0.01
P ₂ O ₅	0.06	0.06	0.06	0.05	0.06	0.05	0.06	0.07	0.06	0.07
H ₂ O	1.27	1.14	1.32	1.54	1.24	1.78	1.56	0.93	1.23	1.34
CO ₂	0.09		0.09			0.11	0.09			
Sum	100.2	101.4	99.5	99.8	99.7	100.1	100.2	99.6	99.3	100.3
Mg#	66.1	65.4	65.1	68.1	66.1	68.0	68.3	64.3	65.5	63.1
FeO*	8.99	9.33	9.22	8.48	9.27	8.53	8.33	9.21	8.99	9.67
Fe ³⁺ /ΣFe	0.28	0.26	0.28	0.22	0.29	0.29	0.20	0.21	0.24	0.24
Trace elements (wt%):										
S	310	560	330	<20	920	560	<20	1010	350	210
Cr	370	362	396	379	376	399	377	333	336	267
Ni	116	123	113	132	145	140	124	102	111	86
Cu	104	89	105	22	98	115	10	95	76	77
Zn	50	55	60	40	54	47	34	72	50	53
Ga	14	15	13	14	14	15	14	15	14	15
Sr	56	55	54	54	54	52	53	65	61	66
Y	27	23	27	19	23	24	24	24	23	27
Zr	44	42	44	34	41	40	40	50	47	53
Li		0.69		0.79		1.05		0.91	1.03	1.06
Sc		45		45		42		43	44	45
Rb		0.06		0.09		0.05		0.04	0.24	0.23
Nb		0.30		0.28		0.29		0.36	0.46	0.59
La		0.94		0.75		0.98		1.21	1.40	1.53
Ce		3.75		2.86		3.67		4.52	4.99	5.46
Nd		4.40		3.47		4.31		5.20	5.37	6.18
Sm		1.82		1.60		1.75		2.08	2.15	2.35
Eu		0.74		0.63		0.72		0.79	0.84	0.95
Gd		2.70		2.35		2.59		2.90	3.10	3.45
Tb		0.51		0.41		0.50		0.54	0.57	0.61
Dy		3.79		3.02		3.62		4.02	4.08	4.25
Ho		0.76		0.62		0.75		0.79	0.82	0.90
Er		2.37		1.90		2.32		2.42	2.54	2.65
Tm		0.34		0.27		0.33		0.36	0.35	0.38
Yb		2.32		1.82		2.28		2.38	2.30	2.50
Lu		0.33		0.27		0.33		0.35	0.34	0.37
Th		0.015		0.012		0.013		0.025	0.027	0.031
U		0.006		0.005		0.004		0.009	0.009	0.008
Th/U		2.54		2.37		3.29		2.88	2.81	3.69
Zr/Nb		140		122		138		139	101	90
La/Nb		3.11		2.70		3.35		3.38	3.05	2.58
Th/Nb		0.049		0.041		0.045		0.071	0.058	0.053
(La/Sm) _n		0.33		0.30		0.36		0.38	0.42	0.42
(Sm/Yb) _n		0.87		0.98		0.85		0.97	1.04	1.04

4. A maximum of 50% crystallization of a parental melt, corresponding to cooling from 1260° to 1170°C, can account for the chemical variability of most elements (except very mobile elements like S, H₂O, and Cu and highly incompatible elements like Th, LREEs, Nb, etc.). The larger variability of mobile elements is clearly an effect of hydrothermal alteration, whereas the larger variability of highly incompatible elements has been previously explained by heterogeneous mantle (e.g., Tual et al., 1985) or multi-stage melting (e.g., Autio et al., 1989).

5. The net chemical consequences of advanced fractional crystallization are decreases in MgO, Al₂O₃, CaO, Cr, and Ni and increases in SiO₂, TiO₂, FeO*, Na₂O, Zr, REE, and other incompatible elements. Concentrations of Cu, Sr, and Co are not drastically changed when the degree of fractional crystallization is small (< 50%).

6. Fractional crystallization cannot significantly change the ratios of highly and moderately incompatible elements (e.g., Nb/Zr) and moderately and mildly incompatible elements (e.g., Zr/Ti).

Chemical Effects of Alteration

Details of the diverse alteration mineralogy of the lower SDC are discussed in Alt et al. (this volume) and Vanko et al. (this volume). The basic chemical changes that accompany the various types of alteration are listed in Table 5.

One possible way to assess the degree of chemical alteration is to determine H₂O⁺ concentrations, because water can only be gained during alteration in these rocks. The problem is that secondary phases have different water contents. For example, talc is formed at low water-rock interaction, but has high water contents and thus obscures the correlation between water contents and degree of alteration.

Figure 5 plots selected elements vs. the degree of alteration with the different rock types represented by different symbols. The weak correlation observed between water content and the degrees of alteration indicates a net gain of water because of the formation of secondary minerals (amphibole, chlorite, talc, etc.). Very high water

Table 4 (continued).

Core, section:	249R-1	249R-1	250R-1	250R-1	251R-1	251R-1	251R-1	251R-1	252R-1	252R-1
Interval (cm):	71–76	0–5	14–21	98–102	12–17	72–76	76–80	105–109	4–8	15–20
Piece no.:	24	1	4	28	4	11	12	20	2	5
Depth (mbsf):	2071.91	2072.68	2080.54	2081.38	2090.02	2090.62	2090.66	2090.95	2099.44	2099.55
Lith. unit:	290	291	291	291	293	293	293	293	293	293
Rock type:	M-POD	M-POCD	M-POCD	M-POCD	M-POCD	M-POCD	M-POCD	M-POCD	M-POCD	M-POCD
Alteration type:	Dark	Dark	Dark	Halo + amph. vein + dark	Patch + vugs	Dark	Green (patch?)	Dark	Patch + dark	Patch + vugs
Group:	D	D	D	H	P	D	P	D	P	P
Alteration (%):	30	10	15	40	60	30	60	20	60	80
Major elements (wt%):										
SiO ₂	50.3	49.4	49.7	49.4	48.5	48.6	48.4	48.7	48.1	48.9
TiO ₂	0.84	0.87	0.86	0.85	0.67	0.72	0.72	0.78	0.76	0.54
Al ₂ O ₃	16.4	16.1	15.9	15.6	15.5	16.5	15.8	16.3	16.2	15.1
FeO	6.43	6.82	6.81	6.45	7.31	6.68	6.82	6.31	6.80	6.95
Fe ₂ O ₃	2.28	2.07	2.02	2.23	1.88	1.99	1.91	2.33	1.88	2.11
MnO	0.15	0.16	0.16	0.16	0.14	0.15	0.15	0.15	0.14	0.15
MgO	8.80	8.25	8.27	8.65	9.83	9.45	9.46	9.23	10.01	9.65
CaO	13.4	13.1	13.0	12.8	12.5	13.0	13.0	13.4	12.9	12.3
Na ₂ O	1.85	1.88	1.93	1.93	2.02	1.57	1.60	1.70	1.61	1.96
K ₂ O	<0.01	<0.01	<0.01	0.01	0.01	<0.01	<0.01	<0.01	<0.01	0.02
P ₂ O ₅	0.06	0.06	0.06	0.06	0.05	0.05	0.05	0.06	0.05	0.04
H ₂ O	1.35	0.88	1.14	1.63	2.52	1.91	1.64	1.47	2.07	1.44
CO ₂				0.11	0.1		0.1	0.06	0.07	0.11
Sum	101.8	99.6	99.8	99.9	101.0	100.5	99.6	100.5	100.6	99.3
Mg#	67.3	65.3	65.5	66.9	68.4	68.8	68.7	68.5	70.0	68.4
FeO*	8.48	8.68	8.63	8.45	9.00	8.47	8.54	8.41	8.49	8.85
Fe ³⁺ /ΣFe	0.24	0.21	0.21	0.24	0.19	0.21	0.20	0.25	0.20	0.21
Trace elements (ppm):										
S	100	970	570	70	<20	1460	20	310	120	<20
Cr	332	326	325	386	355	366	316	333	319	375
Ni	121	109	104	111	147	160	140	139	167	147
Cu	38	86	82	9	6	93	18	171	43	6
Zn	38	69	66	44	49	49	39	42	42	49
Ga	15	15	16	16	13	14	14	14	15	12
Sr	59	66	61	59	60	51	53	54	50	61
Y	22	21	22	25	21	20	23	24	24	19
Zr	43	46	42	45	34	36	36	39	38	29
Li	0.98	0.96	1.26		1.88	1.44				0.27
Sc	41	43	42		38	44				37
Rb	0.17	0.15	0.13			0.13				
Nb	0.51	0.40	0.37		0.25	0.32				0.23
La	1.13	1.21	1.18		0.58	0.96				0.54
Ce	4.08	4.40	4.31		2.51	3.52				2.17
Nd	4.64	4.99	4.91		3.12	4.01				2.91
Sm	1.82	1.93	2.00		1.29	1.67				1.12
Eu	0.74	0.77	0.83		0.62	0.69				0.68
Gd	2.60	2.87	2.90		1.93	2.45				1.79
Tb	0.48	0.49	0.53		0.35	0.46				0.34
Dy	3.40	3.38	3.61		2.90	3.12				2.55
Ho	0.71	0.72	0.73		0.61	0.66				0.57
Er	2.18	2.11	2.27		1.85	2.08				1.63
Tm	0.30	0.31	0.32		0.30	0.30				0.23
Yb	2.05	2.03	2.10		1.93	1.94				1.74
Lu	0.29	0.30	0.29		0.30	0.28				0.25
Th	0.030	0.024	<0.02		0.013	<0.02				0.022
U	0.007	0.008	<0.01		0.005	<0.01				0.008
Th/U	4.34	2.93			2.69					2.60
Zr/Nb	83	116	113		136	112				124
La/Nb	2.22	3.06	3.19		2.30	3.03				2.34
Th/Nb	0.059	0.061			0.054					0.094
(La/Sm) _N	0.40	0.41	0.38		0.29	0.37				0.31
(Sm/Yb) _N	0.99	1.06	1.06		0.74	0.96				0.72

Note: See text for sample descriptions and analytical precisions. Group letters H, P, and D explained in text. Lith. unit = lithologic unit. Rock type abbreviations are as follows: S = sparsely phyrlic, M = moderately phyrlic, P = plagioclase, O = olivine, C = clinopyroxene, and D = diabase. act. = actinolite, and amph = amphibole. ND = not determined. Mg# = molar ratio (Mg/[Mg + Fe 0.9]) × 100.

concentrations (up to 6 wt%) as reported from rocks of Leg 140 (Zuleger et al., 1995) have not been observed in Leg 148 diabases.

Following are other observations on chemical trends with percentage of alteration:

1. Possible slight decreases of CaO and SiO₂ and possible increases of MgO (chloritization, Table 5). However, these trends are poorly defined.
2. Variable enrichments and depletions of Na₂O resulting from the formation of secondary albite-oligoclase (gain) and chlorite (loss).
3. Drastic decreases in TiO₂, MnO, Zr, and Ce (and other REEs) in the more altered rocks, which are particularly obvious in the alteration patches.

4. Dramatic decreases in Cu and S, probably because of the breakdown of primary sulfides (e.g., chalcopyrite), and locally redistribution of Cu and S through precipitation of secondary sulfides (cf. Alt et al., 1995).
5. Overall decreases in Zn concentrations from 70 to 30 ppm within the dark diabases with 10%–50% alteration and a possible slight increase in Zn contents within the most extensively altered patches.

Most trends are more obvious if the alteration halos are excluded, suggesting that the particularly complex alteration mineralogy of the halos obscures chemical trends. On Figure 6, many elements (e.g., Ca, Ti, Na, S, Cu, Zn, Zr) show considerable compositional scatter only above about 20% alteration. However, some of the composition-

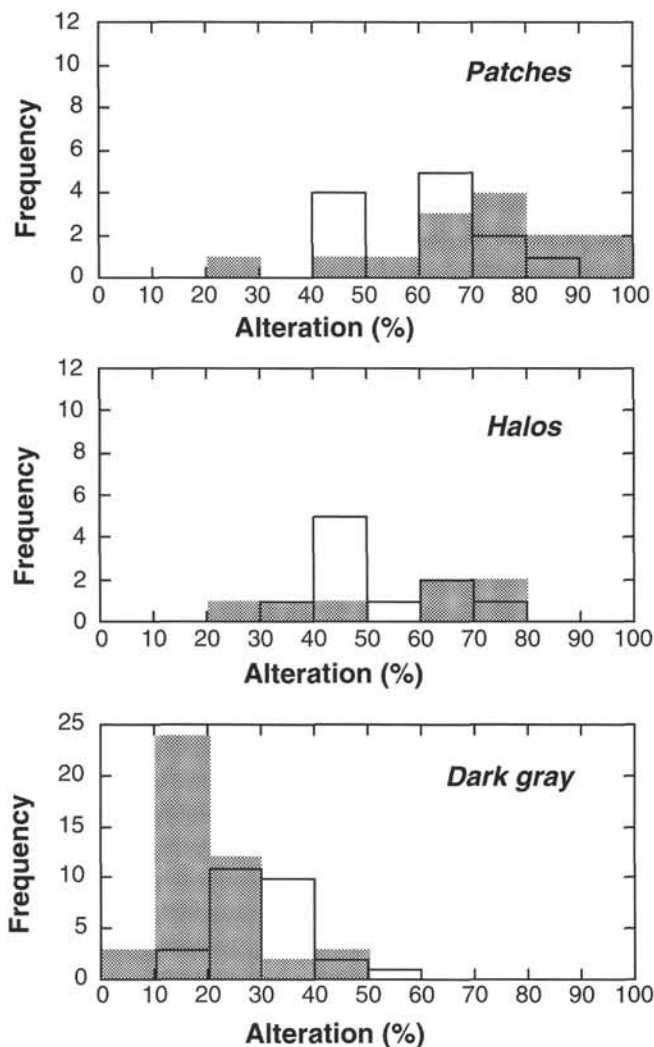


Figure 3. Histograms of degrees of alteration in the different rock types of the lower sheeted dike complex in Hole 504B. Shaded bars = Leg 140 (Zuleger et al., 1995), and open bars = Leg 148 (this work). Note that the background alteration within the dark diabases is slightly higher in Leg 148.

al variability is probably the result of primary magmatic differences in rock chemistry.

Nature of the Patches

One of the most intriguing results of studying the chemistry of the SDC drilled at Site 504 is the peculiar depletion of incompatible elements in the alteration patches. In this paper, we discuss several processes that could be related to the formation and the depleted nature of the patches and try to evaluate the merits and limitations of different models.

Several authors studied the chemistry of alteration patches in the lower SDC in Hole 504B and their findings and conclusions differ in many respects. Zuleger et al. (1995) reported that REEs (and Zr, Ti, Y) are increasingly depleted as the rocks become more altered, and that the depletion is particularly high in alteration patches. Sparks (1995) stated that REEs, Zr, Ti, and Y are not depleted in rocks up to 60% alteration and that the depletions are restricted to alteration patches. Gorton et al. (1995) interpreted variations in REE and Zr as reflecting mantle source heterogeneities and observed significant losses of Cu, Zn, and Ti and some loss of La. Kepezhinskis et al.

(1995) thought that the variable REE depletions represent original magmatic characteristics of the crust. In contrast to the findings of Zuleger et al. (1995), Kepezhinskis et al. (1995) reported slight La and Ce increases with progressive degree of alteration and virtual immobility of the other REEs.

Our results unequivocally support the finding of Zuleger et al. (1995) that REE concentrations are lower in highly altered rocks and are particularly low in alteration patches. This is demonstrated in Figure 6A where REE patterns of increasingly altered rocks are plotted. A remarkable feature is the positive Eu anomaly displayed by the most altered samples. Figure 6B shows the average REE concentrations of dark diabases and alteration patches with filled areas representing the standard deviations. On average, the alteration patches have lower REE concentrations and slightly positive Eu anomalies. There are more chemical differences between patchy and dark diabases. Table 6 summarizes a comparison of the mean chemical compositions of these two rock types. Elements with significant changes are printed in italic style, whereby we defined differences exceeding the standard deviations as significant. Beside the REEs, Nb, Zr, Ti, Cu, Zn, and S also show significant losses, whereas water shows significant gains. Figure 7 shows the compositional differences between patch and dark diabase in the order of increasing degree of depletion. S and Cu are most extensively depleted in the patches followed by the LREEs, Nb, Th, MREEs, Zr, Zn, Eu, HREE, Ti, Mn, P, Fe, Sr, Ca, and Si. Enrichments are indicated only of Mg, Al, Cr, Ni, and H₂O. The REEs (plotted as inset in Fig. 7) show larger depletions in LREE (La, Ce, Nd) as compared to the heavier REEs. Eu displays a smaller degree of depletion than the neighboring elements.

Mobilization of Nominally Immobile Elements

Rare-earth elements and elements of high field strength (Zr, Nb, Ti) are generally considered as being immobile during most alteration processes (e.g., Pearce and Norry, 1979). Gillis et al. (1992) argued that REE concentrations either would not change or would increase during rock alteration at high temperatures. In contrast, Sparks (1995) suggested the mobilization of REEs (and Zr, Ti, and Y) during intensive alteration of the patches in Hole 504B and discussed the possibility that the alteration patches could be a source for the high REE concentrations in high-temperature hydrothermal fluids (e.g., Michard, 1989).

Figure 8 depicts schematic patterns of such a hydrothermal fluid and a hypothetical fluid carrying the REEs lacking in the alteration patches (cf. Fig. 7). In contrast to the marked positive Eu anomaly typical for all high-temperature hydrothermal vent fluids, the "patch fluid" would have a negative Eu-anomaly. As the hydrothermal fluids continuously react with the rocks such that calcic plagioclase, oligoclase, and albite (in order of decreasing fluid temperature) are formed (e.g., Alt et al., 1995), Eu would become more depleted in the fluid in the course of upwelling, thus leading to even more pronounced negative Eu anomalies. This sort of consideration makes a simple relationship between the REE depletion in the alteration patches and the REE enrichment in hydrothermal fluids unlikely.

In general, a mobilization of such large amounts of (nominally immobile) elements is difficult to envision. Chloride complexes would transport the LREEs more efficiently than the HREEs (Wood, 1990, and references therein), but they are unlikely to leach large quantities of REEs unless the water/rock ratios are extremely high (>10⁵, Michard and Albarède, 1986). Carbonate complexes as potential carriers of REEs cannot account for this depletion because the hydrothermal fluids are acidic and hence do not contain sufficient amounts of carbonate or bicarbonate ions. Fluoride complexes would preferentially transport the heavy REEs (Walker and Choppin, 1967) which would cause the opposite trend of what has been observed. Sulfate complexes are important in acidic solution but show little preference between the LREEs and the HREEs (Wood, 1990, and references therein).

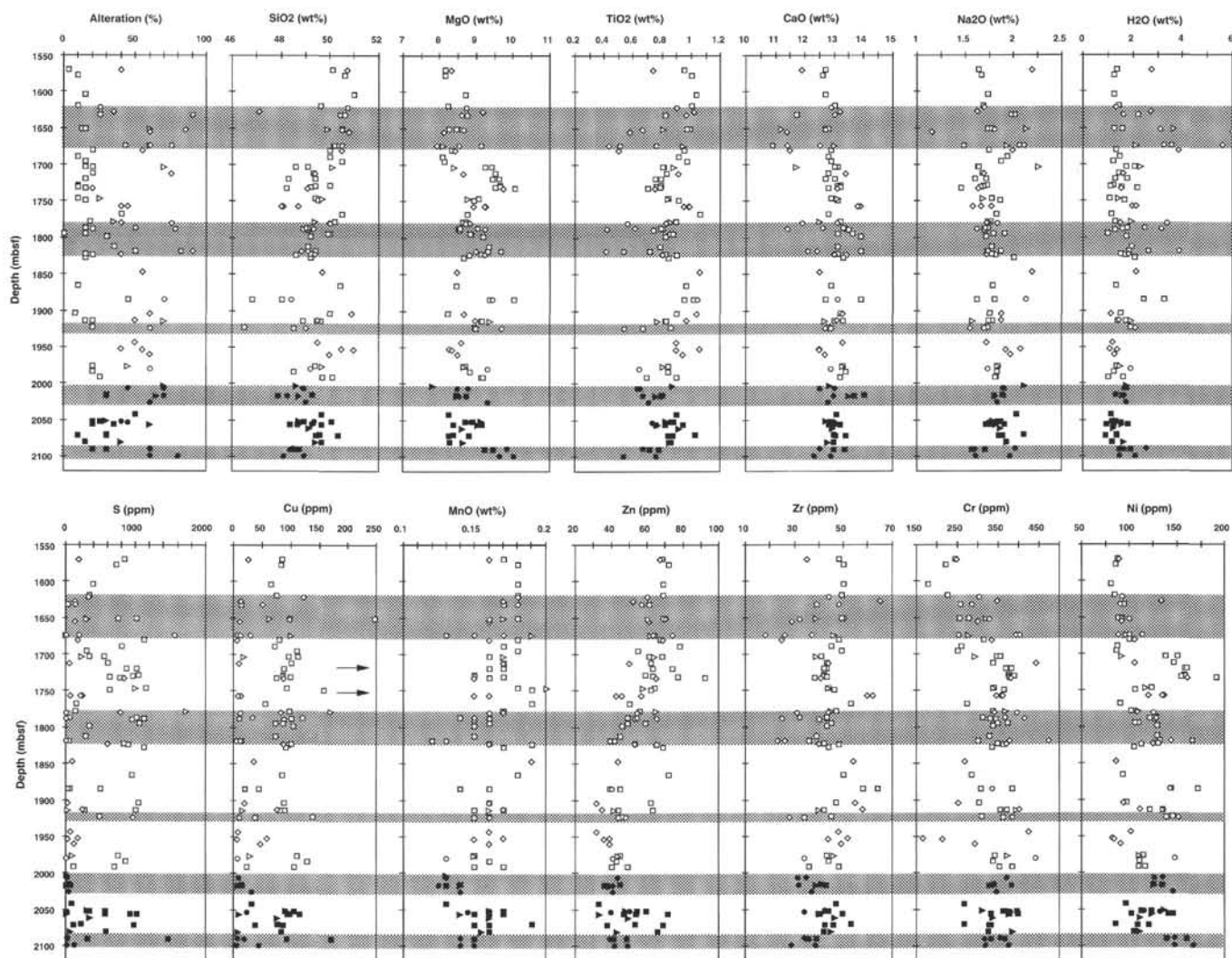


Figure 4. Chemical variation of the lower sheeted dike complex with depth. Open symbols = Leg 140 (Zuleger et al. 1995), and solid symbols = Leg 148 (this work; Alt, Kinoshita, Stokking, et al., 1993). Squares = dark diabases, circles = patches, triangles = halos, and diamonds = light diabases (only Leg 140). Shading marks regions with abundant patches.

Little is known about the mobilities of nominally immobile elements when a rock reacts with very high-temperature fluids (500°C), as was the case for the alteration halos and the alteration patches. It is, however, interesting that the patches are depleted but the halos are not. In short, in view of these theoretical considerations, a profound incompatible element depletion of the patches through alteration is hard to explain.

Mass-balance Calculations

To make a more quantitative approach to assess possible element transports during alteration, we used the mass-balance calculation methods of Gresens (1967) and Grant (1986).

Strict application of mass-balance calculations to the problem of element mobilization in basaltic rocks has shown that in many cases volume changes during metamorphism can account for the changes in REE contents rather than mobility of REEs (Bartley, 1986).

On the other hand epidotes in ophiolites sometimes exhibit nearly quantitative removal of Zr and Y (Schiffman and Smith, 1988). These epidotes are different from other metabasites: they are totally recrystallized into granoblastic textures. This texture and the deple-

tions of Mg, Na, and sometimes Al argue for very high water/rock ratios of about 500 (Schiffman et al., 1990; Nehlig et al., 1994).

Gorton et al. (1995) declined the application of mass-balance calculations to Hole 504B rocks, because of too large primary chemical differences of the dikes. We therefore restrict our mass-balance consideration to one section (Section 140-504B-193R-1) where Zuleger et al. (1995) analyzed a piece of dark diabase adjacent to a virtually completely recrystallized patch. A Grant plot showing the gains and losses in various elements is depicted in Figure 9. If the chemical composition had not been changed, the data would plot along the solid lines, assuming no volume changes or mass changes.

In Figure 9, most elements plot below the solid lines (i.e., would have been mobilized during alteration). The plot indicates gains in H₂O, Rb, and Cr, and virtually no changes in Si, Mg, Al, and Fe. Except Cu and S, elements like Zr, REEs, Nb, and Th would be the most effectively mobilized ones. Another approach to mass transport phenomena is to assume that certain elements are immobile. As discussed earlier, REEs, Zr, Nb, and so on, are commonly thought to be immobile. These elements plot along the dashed line in Figure 9 and the slope of this line is proportional to the volume change of the alteration process. All elements plotting above the dashed line must

Table 5. Simplified chemical effects of various types of alteration.

Uralitization Cpx→Amph		Chloritization Ol/Cpx/Plg→Chl		Albitization Plg→Ab		Epidotization Plg→Epi		Ilmenite-Titanite Ilm→Tit	
Loss	Gain	Loss	Gain	Loss	Gain	Loss	Gain	Loss	Gain
SiO ₂	H ₂ O	SiO ₂	MgO	CaO	Na ₂ O	SiO ₂	CaO	FeO	CaO
CaO		CaO Al ₂ O ₃	H ₂ O	Al ₂ O ₃	SiO ₂		H ₂ O	TiO ₂ (?)	SiO ₂

Note: Cpx = clinopyroxene, Amph = amphibole, Ol = olivine, Plg = plagioclase, Chl = chlorite, Ab = albite, Epi = epidote, Ilm = ilmenite, and Tit = titanite.

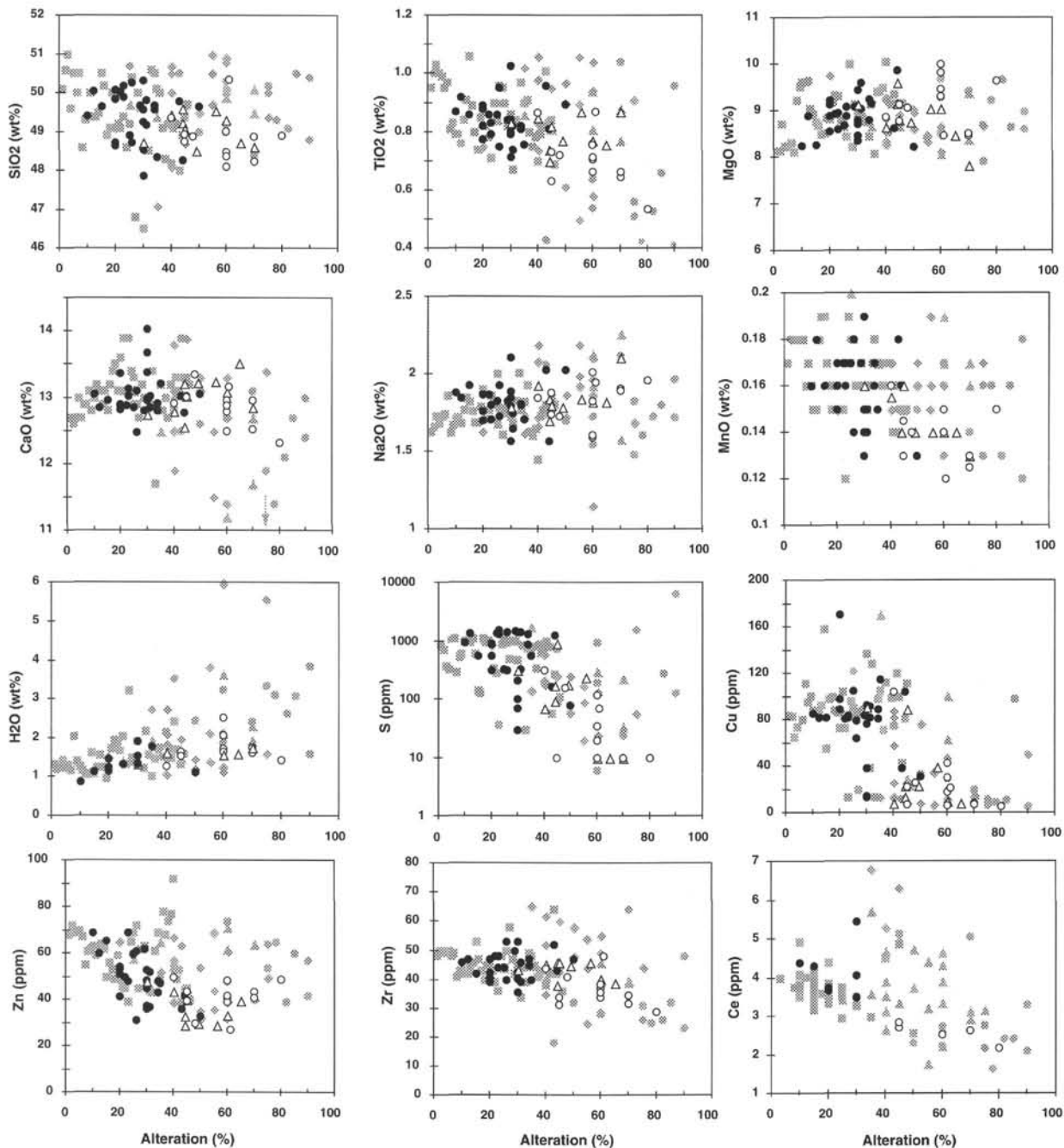


Figure 5. Variation of rock chemical compositions with degree of alteration. Symbols as in Figure 4.

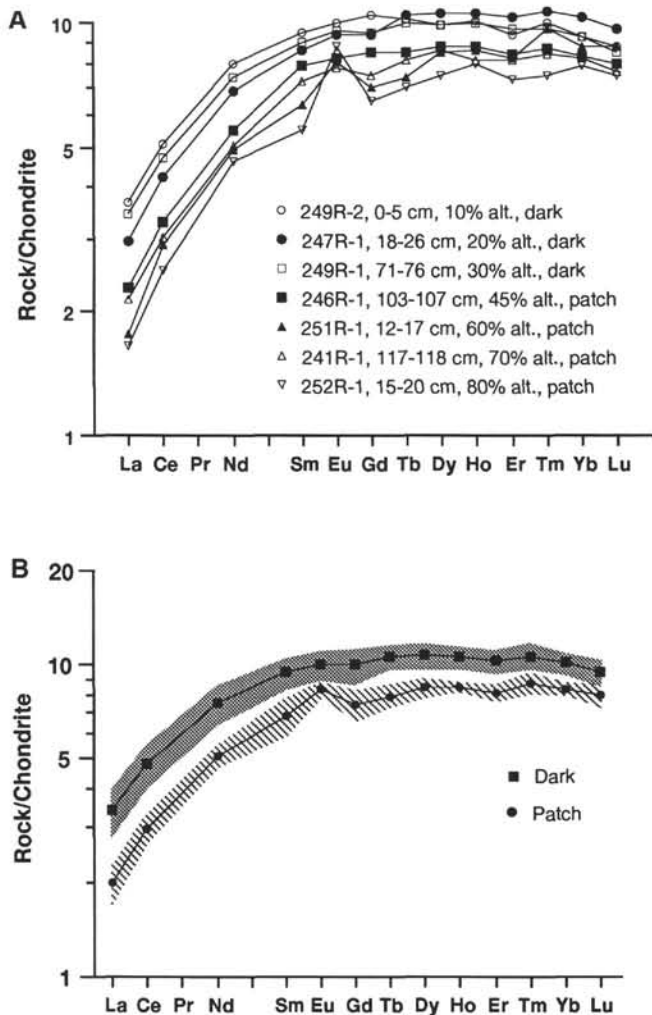


Figure 6. Rare-earth element (REE) patterns of selected samples from Leg 148. **A.** Various extents of REE depletion within the dark diabases and the patches. **B.** Mean REE contents of dark diabases and patches, respectively. The stippled areas represent standard deviation of the mean. Note that patches are significantly depleted in REEs and have positive Eu anomalies.

have been added to the rock. This approach yields volume changes of around 100% which are unrealistic as primary magmatic textures are preserved in many patches. Bartley (1986) considered volume changes of up to 30% as a maximum for rocks showing preservation of primary textures. Gresens's calculations also yield unrealistically high volume factors of up to 2. This holds true not only for the dark/patch pair of Section 140-504B-193R-1 but for many other dark/patch pairs that have been taken into consideration.

We conclude that alteration might be capable of producing depletions in REEs, Y, Ti, Zr, Nb, etc., to some extent, but that the observed dramatic depletion of these elements in the patches through alteration is improbable, especially because the major elements are virtually unchanged. Moreover, alteration halos around amphibole veins have similar alteration mineralogy and some are also intensively altered, but halos do not show the same sort of depletion, suggesting that the chemical depletion of the patches might be of primary nature.

Primary Depletion of the Patches

Zuleger et al. (1995) proposed a primary depletion of the patches through expulsion of late-stage, highly differentiated interstitial melt,

leaving a rock depleted in incompatible elements. This process must have been somehow related to the formation of high porosities that led subsequently to high fluid flows through these more permeable areas. The high fluid flow resulted in intense water-rock interaction and high degree of recrystallization. Evidence for the presence of such highly evolved interstitial melts are provided by small pockets of granophytic quartz and albite with minor clinopyroxene, apatite, and Fe-Ti oxides (Dick, Erzinger, Stokking, et al., 1992). The difficulty with this concept is to find a physically reasonable process for the separation of these melts from the solid residue (i.e., a driving force for the liquids). Exsolution and expansion of volatiles in magmas has been discussed as a possible mechanism in Zuleger et al. (1995). Indeed, volume expansion of volatile-rich magmas and coinciding segregation of gas vesicles has been documented recently in basalts from the Lau Basin (Bloomer, 1994). However, the Lau Basin example may not be strictly comparable to the situation at Site 504, because the primary water contents of these back arc basin basalts were high and the eruption depth relatively shallow. Taking the primitive and depleted nature of Hole 504B basalts into account, the primary water contents must have been very low, maybe in the order of 0.1 or 0.2 wt% (cf. Michael, 1988). The solubility of water in basaltic melts at 1200°C and 1 kbar is as high as 4 wt% (Burnham, 1975). It would thus need at least 95–98 wt% fractional crystallization to get a melt supersaturated in water.

Exsolution of CO₂ could be an alternative mechanism, since the solubility of CO₂ in basaltic melts is low (0.44 ppm/bar; Stolper and Holloway, 1988) and nucleation and growth of CO₂ bubbles starts already at great depths (e.g., Bottinga and Javoy, 1990). However, taking into account the molar volume of CO₂ at 1200°C and 1 kbar, it would take 0.25 to 2.5 wt% CO₂ exsolved to account for a porosity of 2 to 20 vol% (calculated assuming a perfect gas). The primary CO₂ contents are probably lower than 400 ppm (Fine and Stolper, 1986) and therefore such high CO₂ concentrations are unrealistic. Moreover, high degrees of supersaturation result in drastically lower nucleation rates of the CO₂ bubbles, thus inhibiting exsolution and segregation of CO₂ bubbles particularly because ascent velocities of basaltic melts in dikes are high (1 m/s; Delaney and Pollard, 1982).

The amygdules found in many patches are thought to represent primary pore space ranging from 2% to 20%. The subrounded shapes of many amygdules are similar to gas vesicles and exsolution of gas could potentially drive out interstitial melt leading to the depleted nature of the patches. However, because of the simple calculations made above we feel that volatile-rich magma expansion is not very likely to occur in dikes of the oceanic crust. We therefore favor the possibility that the amygdules represent primary pore space produced by shrinkage during crystallization of the melt and subsequent cooling of the rock. The idea of late-stage melt expulsion must not necessarily be rejected, if these interstitial liquids were just squeezed out mechanically (e.g., during dike compaction).

This puzzling question remains: Why are the patches depleted in incompatible elements and highly altered at the same time? We do not favor alteration to account for the depletion and we hardly can think of a reasonable physical process that may have expelled or squeezed out late-stage interstitial melts.

Yet another problem with the late-stage melts as an explanation is that they would be enriched in Zr and REEs but not in Ti, which would decrease after FeTi-oxides join the fractionating mineral assemblage (Fig. 10). The observed simultaneous depletion of Ti and Zr, REEs, Nb, etc. is therefore difficult to explain by removal of late-stage melts. A third possibility would be to regard the patches as xenocrystic material that was incorporated in the melt upon dike intrusion. If the material were highly altered, water-rich diabases or gabbros, this could account for both the high alteration and the chemically distinct (depleted) compositions. Petrographic studies of the patches, however, do not support a xenocrystic nature of the patches, since clear textural changes across the patch margins have never been observed.

Table 6. Comparison of compositional range and average compositions of dark diabases and patchy diabases.

	Dark (N = 28, 9)				Patch (N = 12, 5)			
	Min.	Max.	Mean	SD	Min.	Max.	Mean	SD
Major elements (wt%):								
SiO ₂	47.88	50.33	49.42	0.66	48.11	50.34	48.86	0.59
TiO ₂	0.72	1.03	0.84	0.07	0.54	0.87	0.71	0.09
Al ₂ O ₃	13.78	17.14	15.44	0.78	14.85	17.30	16.04	0.75
FeO*	7.50	9.75	8.75	0.53	7.78	9.00	8.45	0.43
MnO	0.13	0.19	0.16	0.02	0.12	0.16	0.14	0.01
MgO	8.24	9.88	8.87	0.41	8.47	10.01	9.13	0.53
CaO	12.48	14.03	13.03	0.30	12.33	13.35	12.87	0.29
Na ₂ O	1.57	2.11	1.82	0.13	1.60	2.02	1.83	0.14
P ₂ O ₅	0.03	0.07	0.05	0.01	0.04	0.06	0.05	0.01
H ₂ O	0.30	1.91	1.01	0.45	0.68	2.52	1.58	0.47
Trace elements (ppm):								
S	20	1538	745	538	20	308	118	106
Cr	205	399	312	49	247	383	343	43
Ni	86	160	120	19	101	167	136	17
Cu	14	171	80	31	6	104	25	27
Zn	31	72	50	11	27	50	41	7
Ga	13	16	15	1	12	16	14	1
Sr	48	66	57	5	50	61	56	3
Y	19	29	23	2	16	27	21	3
Zr	36	53	45	5	29	48	37	6
Li	0.69	1.44	1.06	0.21	0.27	1.88	0.92	0.59
Sc	34	47	41	3	37	48	41	4
Rb	0.04	0.23	0.12	0.06	0.09	0.11	0.10	0.01
Nb	0.29	0.59	0.38	0.10	0.23	0.28	0.26	0.02
La	0.94	1.53	1.12	0.19	0.54	0.75	0.66	0.09
Ce	3.49	5.46	4.13	0.63	2.17	2.86	2.58	0.26
Nd	4.01	6.18	4.77	0.65	2.91	3.47	3.20	0.21
Sm	1.67	2.35	1.92	0.20	1.12	1.60	1.39	0.19
Eu	0.69	0.95	0.77	0.08	0.60	0.68	0.64	0.03
Gd	2.15	3.45	2.75	0.35	1.79	2.35	2.05	0.21
Tb	0.46	0.61	0.51	0.04	0.34	0.41	0.38	0.03
Dy	3.24	4.25	3.68	0.32	2.55	3.02	2.88	0.19
Ho	0.66	0.90	0.75	0.06	0.57	0.62	0.60	0.02
Er	2.11	2.65	2.31	0.17	1.63	1.90	1.82	0.10
Tm	0.30	0.38	0.33	0.03	0.23	0.30	0.27	0.02
Yb	2.03	2.50	2.22	0.17	1.74	1.93	1.83	0.07
Lu	0.28	0.37	0.32	0.03	0.25	0.30	0.27	0.02
Th	0.013	0.031	0.022	0.007	0.012	0.022	0.016	0.004
U	0.004	0.009	0.007	0.002	0.005	0.008	0.006	0.001

Notes: Numbers in italic typeface indicate elements that are significantly different in patches. N = number of XRF and ICP-MS analyses, respectively. Min. = minimum, Max. = maximum, and SD = standard deviation.

Zn, Cu, and S Depletions

Dick, Erzinger, Stokking, et al. (1992) reported a generally decreasing trend of Zn concentrations in the lower part of the SDC in 504B (>1600 mbsf), the so-called "reaction zone." At the same time Cu and S show various extents of depletion on the meter scale and have a crude bimodal distribution. This was explained by Zuleger et al. (1995) and Sparks (1995) as evidence for silicate-controlled behavior of Zn and sulfide-controlled behavior of Cu and S. In rocks from Leg 148, Zn and Cu show a poor covariation and Cu exhibits a bimodal distribution (Fig. 11). Most of the dark diabases have high Cu concentrations around 80 ppm, which is close to the Cu concentrations of fresh lavas from Hole 504B (Hubberten et al., 1983). Most of the patches and halos have low Zn and Cu concentrations, with Cu being more extensively leached than Zn.

Simultaneous Cu and Zn depletion are known from many ophiolites and such base-metal depleted zones have been referred to as reaction or root zones of hydrothermal fluids (e.g., Richardson et al., 1987; Schiffman et al., 1990; Nehlig et al., 1994). The base-metal depletion in ophiolites, however, occur in epidiosites which are extremely altered and are often intercalated with more normal greenschist diabases. These epidiosites are thought to be conduits for extremely high fluid flow, often parallel to dike margins (e.g., Nehlig et al., 1994). A general Zn depletion as observed in the lower SDC of Hole 504B has been reported by Harper et al. (1988) from the basal SDC of the Josephine ophiolite.

Alt et al. (1995) proposed that sulfide dissolution, sulfide precipitation and sulfate formation occurring all over the lower SDC are responsible for the perplexing pattern of depth variation of Cu and S. In the section drilled during Leg 148, Cu and S show similar behavior

to that in the upper sections. The general trend of progressive Zn depletion with depth from 1600 to 2000 mbsf changes somewhat in the Leg 148 section (2000–2111 mbsf). Although low Zn contents similar to the overlying dikes are still present, higher Zn contents also occur, particularly below 2050 mbsf. This general trend is displayed by our data and the "shipboard data set" of Leg 148 (Alt, Kinoshita, Stokking, et al., 1993). On the diagram of Zn vs. degree of alteration (Fig. 5), Zn contents of dark diabases and halos generally decrease, but increase in the patches. In our opinion, two explanations for such a behavior of Zn are possible: first, a phase in the patches retains Zn, or more likely, takes up Zn (lost during alteration of the dark diabases) from hydrothermal fluids, and second, the patches are altered at high temperatures where the solubility of Zn is decreased. The latter possibility was also proposed by Sparks (1995) on the basis of results of Seyfried and Janecky's (1985) leaching experiments, which indicated a maximum solubility of Zn and Cu between 375° and 400°C and markedly decreased solubility at higher temperatures. This could mean that the rocks of the SDC were altered by pervasive fluids of optimal temperature for Zn leaching (375°–400°C) in depths where the Zn depletion is most obvious (1700–2000 mbsf). Trends of increasing ¹⁸O depletion continue to the final depth of Leg 148, suggesting that temperatures of pervasive alteration are indeed higher than in the cores recovered during Leg 140 (Alt et al., this volume).

CONCLUSION

Rocks of the lower SDC drilled during Leg 148 (2000–2111 mbsf) exhibit similar chemical characteristics to those previously recovered from Hole 504B. They are also highly depleted in incom-

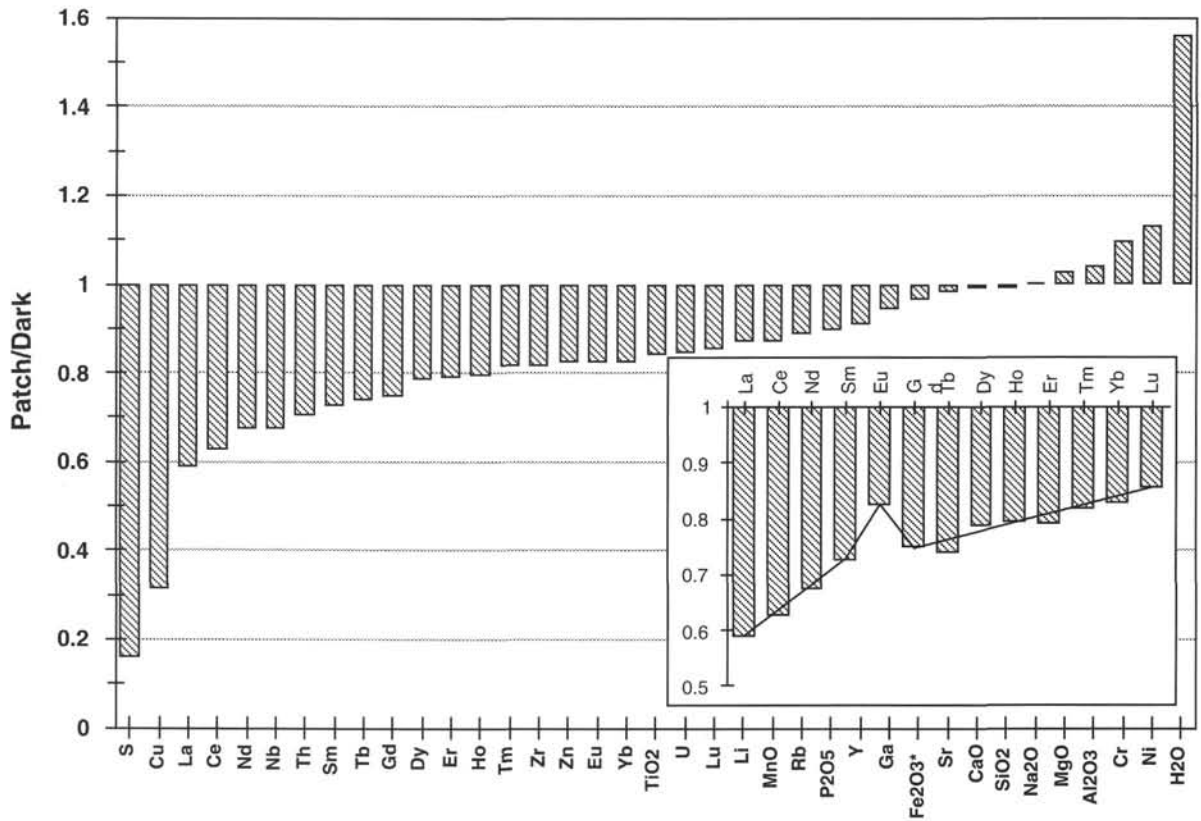


Figure 7. Bar chart, showing average element concentrations in alteration patches divided by the average concentrations in dark diabases in order of increasing depletion. Numbers < 1 indicate depletion (loss), whereas numbers > 1 indicate enrichment (gain). The inset shows the same sort of diagram for the REEs.

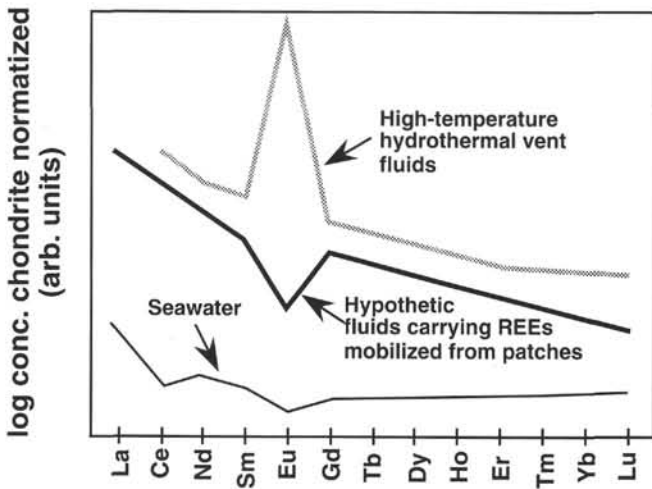


Figure 8. Schematic sketch, demonstrating the difference in REE pattern of hydrothermal fluids and a hypothetical fluid that transports the REEs mobilized from patches. Seawater pattern is shown for reference. Conc. = concentration, and arb. units = arbitrary units. See text for discussion.

patible elements and show a small range in chemical compositions, most of which can be explained by moderate degrees of magmatic differentiation.

A crude sawtooth pattern in the depth variation of Zr, Ti, and Ni, which is most obvious between 1900 and 2111 mbsf, could be inter-

preted as magmatic trends suggesting intrusions of multiple dike packets.

Hydrothermal alteration in the lowermost section is generally more intense than in the section above. The effects of this alteration on the rock chemistry are slight gains of MgO and H₂O and losses of CaO, TiO₂, and SiO₂.

Alteration halos and alteration patches are widespread in the lower SDC. Alteration patches are most abundant from 2000 to 2030 mbsf and between 2085 and 2111 mbsf, where average grain sizes are large, which promotes high alteration of the interior parts of dike packets. The alteration halos show no systematic chemical trends and no clear relationship to the degree of alteration.

In contrast to alteration halos, patches of intense alteration are significantly depleted in REE, Zr, Nb, Ti, etc., and exhibit positive Eu anomalies. Theoretical considerations and mass-balance calculations indicate that this depletion is probably not solely the consequence of intensive alteration, but rather reflects primary differences between the patches and the neighboring diabases. It remains unclear how such differences could be related to magmatic differentiation processes within the dikes.

The alteration patches are significantly enriched in H₂O and highly depleted in Cu (Zn) and S. This makes the lower SDC a possible source for base-metal deposits in the oceanic crust.

Regardless of whether or not the REE depletions of the patches are a matter of alteration, the patches cannot be simply regarded as sources for the REEs in high-temperature hydrothermal fluids. If hydrothermal fluids inherited their REEs inventory solely during formation of the patches, they would have negative Eu anomalies instead of positive ones.

The questions of the formation of alteration patches, their mineralogical (but not chemical) similarity to alteration halos, and the pe-

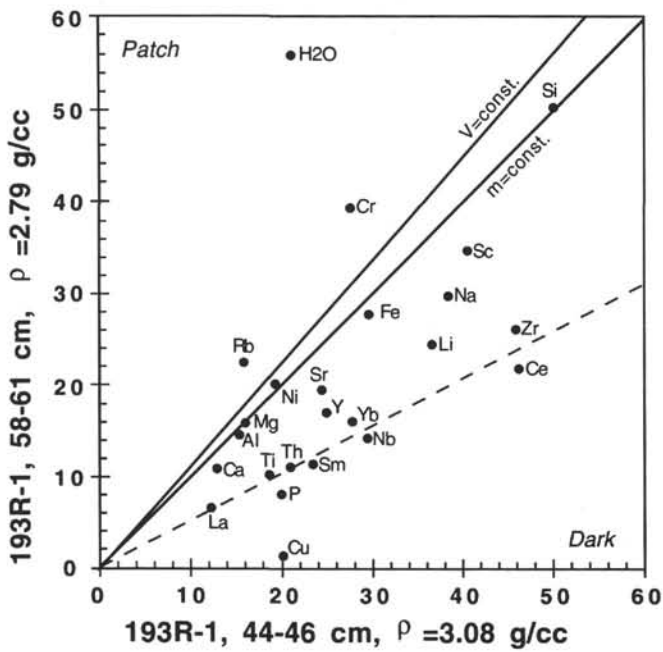


Figure 9. Grant plot, after Grant (1986), showing the difference between a patch (Sample 140-504B-193R-1, 58–61 cm) and a neighboring dark diabase (Sample 140-504B-193R-1, 44–46 cm). V = volume, m = mass, and ρ = pycnometric density. See text for details.

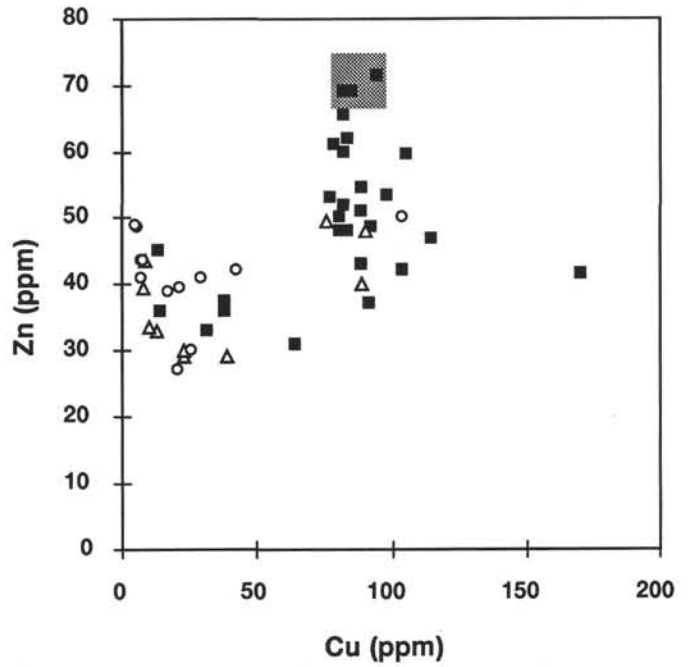


Figure 11. Zn vs. Cu for lower SDC rocks of Leg 148. Symbols as in Figure 4. Shading marks the approximate primary range of Hole 504B lavas.

cular depletion in nominally immobile elements remains largely unanswered and needs further attention.

ACKNOWLEDGMENTS

We thank M. Grünhäuser, H.-G. Plessen, H. Rothe, and R. Zier for their cordial assistance in doing the chemical analyses. The numerous discussions with E. Zuleger have been particularly helpful. The paper benefitted from a review by P. Schiffman. This study was in part supported by Grant No. Er 123/7-1 of the Deutsche Forschungsgemeinschaft (DFG) to J.E., and by grants from JOI-USSAC to J.C.A.

REFERENCES

Alt, J.C., Anderson, T.F., Bonnell, L., and Muehlenbachs, K., 1989. Mineralogy, chemistry, and stable isotopic compositions of hydrothermally altered sheeted dikes: ODP Hole 504B, Leg 111. *In* Becker, K., Sakai, H., et al., *Proc. ODP, Sci. Results*, 111: College Station, TX (Ocean Drilling Program), 27–40.

Alt, J.C., and Emmermann, R., 1985. Geochemistry of hydrothermally altered basalts: Deep Sea Drilling Project Hole 504B. *In* Anderson, R.N., Honnorez, J., Becker, K., et al., *Init. Repts. DSDP*, 83: Washington (U.S. Govt. Printing Office), 249–262.

Alt, J.C., Honnorez, J., Laverne, C., and Emmermann, R., 1986. Hydrothermal alteration of a 1 km section through the upper oceanic crust, Deep Sea Drilling Project Hole 504B: mineralogy, chemistry, and evolution of seawater-basalt interactions. *J. Geophys. Res.*, 91:10309–10335.

Alt, J.C., Kinoshita, H., Stokking, L.B., et al., 1993. *Proc. ODP, Init. Repts.*, 148: College Station, TX (Ocean Drilling Program).

Alt, J.C., Laverne, C., and Muehlenbachs, K., 1985. Alteration of the upper oceanic crust: mineralogy and processes in Deep Sea Drilling Project Hole 504B, Leg 83. *In* Anderson, R.N., Honnorez, J., Becker, K., et al., *Init. Repts. DSDP*, 83: Washington (U.S. Govt. Printing Office), 217–247.

Alt, J.C., Zuleger, E., and Erzinger, J.A., 1995. Mineralogy and stable isotopic compositions of the hydrothermally altered lower sheeted dike complex, Hole 504B, Leg 140. *In* Erzinger, J., Becker, K., Dick, H.J.B., and Stokking, L.B. (Eds.), *Proc. ODP, Sci. Results*, 137/140: College Station, TX (Ocean Drilling Program), 155–166.

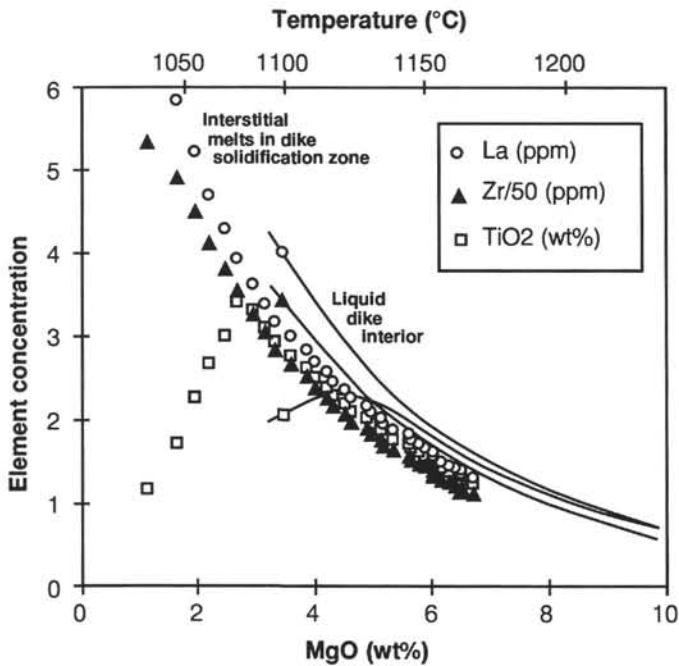


Figure 10. Trends of magmatic differentiation within a solidification zone, calculated using the program of Nielsen (1990). The model assumes a parental melt composition of 10 wt% MgO, 0.7 wt% TiO₂, 30 ppm Zr, and 0.8 ppm La. Note that Ti concentrations would decrease after a certain amount of crystallization (about 80%), whereas Zr and REEs would continuously increase. The model assumes the amount of fractionation occurring within the solidification zone before recharge to be 70% (cf. Nielsen, 1990). Symbols represent compositions of interstitial melts in a hypothetical solidification zone. Solid lines represent compositions of the melts in the dike interior where no crystallization takes place. The kink in the Ti trend is at 80 wt% of crystallization.

- Autio, L.K., and Rhodes, J.M., 1983. Costa Rica Rift Zone basalts: geochemical and experimental data from a possible example of multistage melting. *In* Cann, J.R., Langseth, M.G., Honnorez, J., Von Herzen, R.P., White, S.M., et al., *Init. Repts. DSDP*, 69: Washington (U.S. Govt. Printing Office), 729–745.
- Autio, L.K., Sparks, J.W., and Rhodes, J.M., 1989. Geochemistry of Leg 111 basalts: intrusive feeders for highly depleted pillows and flows. *In* Becker, K., Sakai, H., et al., *Proc. ODP, Sci. Results*, 111: College Station, TX (Ocean Drilling Program), 3–16.
- Barrett, T.J., 1983. Strontium- and lead-isotope composition of some basalts from Deep Sea Drilling Project Hole 504B, Costa Rica Rift, Legs 69 and 70. *In* Cann, J.R., Langseth, M.G., Honnorez, J., Von Herzen, R.P., White, S.M., et al., *Init. Repts. DSDP*, 69: Washington (U.S. Govt. Printing Office), 643–650.
- Bartley, J.M., 1986. Evaluation of REE mobility in low-grade metabasalts using mass-balance calculations. *Nor. Geol. Tidsskr.*, 66:145–152.
- Becker, K., Foss, G., et al., 1992. *Proc. ODP, Init. Repts.*, 137: College Station, TX (Ocean Drilling Program).
- Bloomer, S.H., 1994. Origin of segregation vesicles in volcanic rocks from the Lau Basin, Leg 135. *In* Hawkins, J., Parson, L., Allan, J., et al., *Proc. ODP, Sci. Results*, 135: College Station, TX (Ocean Drilling Program), 615–623.
- Boström, K., and Bach, W., 1995. Trace element determinations by X-ray fluorescence analysis: advantages, limitations, and alternatives. *In* Batiza, R., Storms, M.A., and Allan, J.F. (Eds.), *Proc. ODP, Sci. Results*, 142: College Station, TX (Ocean Drilling Program), 61–68.
- Bottinga, Y., and Javoy, M., 1990. Mid-ocean ridge basalt degassing: bubble nucleation. *J. Geophys. Res.*, 95:5125–5131.
- Bryan, W.B., Thompson, G., Frey, F.A., and Dickey, J.S., 1976. Inferred geologic settings and differentiation in basalts from the Deep Sea Drilling Project. *J. Geophys. Res.*, 81:4285–4304.
- Burnham, C.W., 1975. Waters and magmas: a mixing model. *Geochim. Cosmochim. Acta*, 39:1077–1084.
- Delaney, P.T., and Pollard, D.P., 1982. Solidification of basaltic magma during flow in a dike. *Am. J. Sci.*, 282:856–885.
- Detrick, R., Collins, J., Stephen, R., and Swift, S., 1994. In situ evidence for the nature of the seismic layer 2/3 boundary in oceanic crust. *Nature*, 370:288–290.
- Dick, H.J.B., Erzinger, J., Stokking, L.B., et al., 1992. *Proc. ODP, Init. Repts.*, 140: College Station, TX (Ocean Drilling Program).
- Emmertmann, R., 1985. Basement geochemistry, Hole 504B. *In* Anderson, R.N., Honnorez, J., Becker, K., et al., *Init. Repts. DSDP*, 83: Washington (U.S. Govt. Printing Office), 183–199.
- Etoubleau, J., Corre, O., Joron, J.L., Bougault, H., and Treuil, M., 1983. Costa Rica Rift: variably depleted basalts in the same hole. *In* Cann, J.R., Langseth, M.G., Honnorez, J., Von Herzen, R.P., White, S.M., et al., *Init. Repts. DSDP*, 69: Washington (U.S. Govt. Printing Office), 765–773.
- Fine, G., and Stolper, E., 1986. Dissolved carbon dioxide in basaltic glasses: concentrations and speciation. *Earth Planet. Sci. Lett.*, 76:263–278.
- Garbe-Schoenberg, C.-D., 1993. Simultaneous determination of thirty-seven trace elements in twenty-eight international rock standards by ICP-MS. *Geostand. Newsl.*, 17:81–97.
- Gillis, K.M., Ludden, J.N., and Smith, A.D., 1992. Mobilization of REE during crustal aging in the Troodos Ophiolite, Cyprus. *Chem. Geol.*, 98:71–86.
- Gorton, M.P., Schandl, E.S., and Naldrett, A.J., 1995. Platinum group element (PGE) concentrations in a sheeted dike complex and geochemical changes during alteration of the lowermost part of a 2-km-thick oceanic crust, Hole 504B. *In* Erzinger, J., Becker, K., Dick, H.J.B., and Stokking, L.B. (Eds.), *Proc. ODP, Sci. Results*, 137/140: College Station, TX (Ocean Drilling Program), 199–206.
- Govindaraju, K., 1994. 1994 compilation of working values and sample description for 383 geostandards. *Geostand. Newsl.*, 18.
- Grant, J.A., 1986. The isocon diagram—a simple solution to Gresens's equation for metasomatic alteration. *Econ. Geol.*, 81:1976–1982.
- Gresens, R.L., 1967. Composition-volume relationships of metasomatism. *Chem. Geol.*, 2:47–65.
- Harper, G.D., Bowman, J.R., and Kuhns, R., Jr., 1988. A fluid, chemical, and stable isotope study of subseafloor metamorphism of the Josephine Ophiolite, California-Oregon. *J. Geophys. Res.*, 93:4625–4656.
- Hey, R., Johnson, G.L., and Lowrie, A., 1977. Recent plate motions in the Galapagos area. *Geol. Soc. Am. Bull.*, 88:1385–1403.
- Hobart, M.A., Langseth, M.G., and Anderson, R.N., 1985. A geothermal and geophysical survey on the south flank of the Costa Rica Rift: Sites 504 and 505. *In* Anderson, R.N., Honnorez, J., Becker, K., et al., *Init. Repts. DSDP*, 83: Washington (U.S. Govt. Printing Office), 379–404.
- Hofmann, A.W., 1988. Chemical differentiation of the Earth: the relationship between mantle, continental crust, and oceanic crust. *Earth Planet. Sci. Lett.*, 90:297–314.
- Hubberten, H.-W., Emmertmann, R., and Puchelt, H., 1983. Geochemistry of basalts from Costa Rica Rift Sites 504 and 505 (Deep Sea Drilling Project Legs 69 and 70). *In* Cann, J.R., Langseth, M.G., Honnorez, J., Von Herzen, R.P., White, S.M., et al., *Init. Repts. DSDP*, 69: Washington (U.S. Govt. Printing Office), 791–803.
- Jenner, G.A., Longerich, H.P., Jackson, S.E., and Fryer, B.J., 1990. ICP-MS: a powerful tool for high-precision trace-element analysis in earth sciences: evidence from analysis of selected U.S.G.S. reference samples. *Chem. Geol.*, 83:133–148.
- Jochum, K.P., Seufert, H.M., and Thirlwal, M.F., 1990. Multi-element analysis of 15 international standard rocks by isotope-dilution spark source mass spectrometry. *Geostand. Newsl.*, 14:469–473.
- Kempton, P.D., Autio, L.K., Rhodes, J.M., Holdaway, M.J., Dungan, M.A., and Johnson, P., 1985. Petrology of basalts from Hole 504B, Deep Sea Drilling Project, Leg 83. *In* Anderson, R.N., Honnorez, J., Becker, K., et al., *Init. Repts. DSDP*, 83: Washington (U.S. Govt. Printing Office), 129–164.
- Kepezhinskas, P.K., Sorokina, N.A., Mamontova, S.A., and Savichev, A.T., 1995. Rare-earth and large-ion lithophile (Sr and Ba) element geochemistry of diabase dikes, Hole 504B, Costa Rica Rift, Leg 140. *In* Erzinger, J., Becker, K., Dick, H.J.B., and Stokking, L.B. (Eds.), *Proc. ODP, Sci. Results*, 137/140: College Station, TX (Ocean Drilling Program), 107–116.
- Kusakabe, M., Shibata, T., Yamamoto, M., Mayeda, S., Kagami, H., Honma, H., Masuda, H., and Sakai, H., 1989. Petrology and isotope characteristics (H, O, S, Sr, and Nd) of basalts from Ocean Drilling Project Hole 504B, Leg 111, Costa Rica Rift. *In* Becker, K., Sakai, H., et al., *Proc. ODP, Sci. Results*, 111: College Station, TX (Ocean Drilling Program), 47–60.
- Laverne, C., Vanko, D.A., Tartarotti, P., and Alt, J.C., 1995. Chemistry and geothermometry of secondary minerals from the deep sheeted dike complex, Hole 504B. *In* Erzinger, J., Becker, K., Dick, H.J.B., and Stokking, L.B. (Eds.), *Proc. ODP, Sci. Results*, 137/140: College Station, TX (Ocean Drilling Program), 167–190.
- Marsh, N.G., Tarney, J., and Hendry, G.L., 1983. Trace element geochemistry of basalts from Hole 504B, Panama Basin, Deep Sea Drilling Project Legs 69 and 70. *In* Cann, J.R., Langseth, M.G., Honnorez, J., Von Herzen, R.P., White, S.M., et al., *Init. Repts. DSDP*, 69: Washington (U.S. Govt. Printing Office), 747–763.
- Michael, P.J., 1988. The concentration, behavior and storage of H₂O in the suboceanic mantle: implications for mantle metasomatism. *Geochim. Cosmochim. Acta*, 52:555–566.
- Michard, A., 1989. Rare earth element systematics in hydrothermal fluids. *Geochim. Cosmochim. Acta*, 53:745–750.
- Michard, A., and Albarède, F., 1986. The REE content of some hydrothermal fluids. *Chem. Geol.*, 55:51–60.
- Natland, J.H., Adamson, A.C., Laverne, C., Melson, W.G., and O'Hearn, T., 1983. A compositionally nearly steady-state magma chamber at the Costa Rica Rift: evidence from basalt glass and mineral data, Deep Sea Drilling Project Sites 501, 504, and 505. *In* Cann, J.R., Langseth, M.G., Honnorez, J., Von Herzen, R.P., White, S.M., et al., *Init. Repts. DSDP*, 69: Washington (U.S. Govt. Printing Office), 811–858.
- Nehlig, P., Juteau, T., Bendel, V., and Cotten, J., 1994. The root zone of oceanic hydrothermal systems: constraints from the Samail ophiolite (Oman). *J. Geophys. Res.*, 99:4703–4713.
- Nielsen, R.L., 1990. Simulation of igneous differentiation processes. *In* Nicholls, J., and Russell, J.K. (Eds.), *Modern Methods of Igneous Petrology: Understanding Magmatic Processes*. *Rev. Mineral.*, 24:65–105.
- Pearce, J.A., and Norry, M.J., 1979. Petrogenetic implications of Ti, Zr, Y and Nb variations in volcanic rocks. *Contrib. Mineral. Petrol.*, 69:33–47.
- Richardson, C.J., Cann, J.R., Richards, H.G., and Cowan, J.G., 1987. Metal-depleted root zones of the Troodos ore-forming hydrothermal systems, Cyprus. *Earth Planet. Sci. Lett.*, 84:243–253.
- Schiffman, P., Bettison, L.A., and Smith, B.M., 1990. Mineralogy and geochemistry of epidosites from the Solea Graben, Troodos Ophiolite, Cyprus. *In* Malpas, J., Moores, E., Panayiotou, A., and Xenophontos, C. (Eds.), *Ophiolites: Oceanic Crustal Analogues*. *Proc. Symp. "Troodos 1987"*. *Min. Agr. Nat. Resour., Nicosia, Cyprus*, 673–684.
- Schiffman, P., and Smith, B.M., 1988. Petrology and oxygen isotope geochemistry of a fossil seawater hydrothermal system within the Solea

- Graben, northern Troodos ophiolite, Cyprus. *J. Geophys. Res.*, 93:4612–4624.
- Seyfried, W.E., Jr., and Janecky, D.R., 1985. Heavy metal and sulfur transport during subcritical and supercritical hydrothermal alteration of basalt: influence of fluid pressure and basalt composition and crystallinity. *Geochim. Cosmochim. Acta*, 49:2545–2560.
- Shimizu, H., Mori, K., and Masuda, A., 1989. REE, Ba, and Sr abundances and Sr, Nd, and Ce isotopic ratios in Hole 504B basalts, ODP Leg 111, Costa Rica Rift. In Becker, K., Sakai, H., et al., *Proc. ODP, Sci. Results*, 111: College Station, TX (Ocean Drilling Program), 77–83.
- Sparks, J.W., 1995. Geochemistry of the lower sheeted dike complex, Hole 504B, Leg 140. In Erzinger, J., Becker, K., Dick, H.J.B., and Stokking, L.B. (Eds.), *Proc. ODP, Sci. Results*, 137/140: College Station, TX (Ocean Drilling Program), 81–98.
- Stolper, E., and Holloway, J.R., 1988. Experimental determination of the solubility of carbon dioxide in molten basalt at low pressure. *Earth Planet. Sci. Lett.*, 87:397–408.
- Tual, E., Jahn, B.M., Bougault, H., and Joron, J.L., 1985. Geochemistry of basalts from Hole 504B, Leg 83, Costa Rica Rift. In Anderson, R.N., Honnorez, J., Becker, K., et al., *Init. Repts. DSDP*, 83: Washington (U.S. Govt. Printing Office), 201–214.
- Umino, S., 1995. Downhole variations in grain size at Hole 504B: implications for rifting episodes at mid-ocean ridges. In Erzinger, J., Becker, K., Dick, H.J.B., and Stokking, L.B. (Eds.), *Proc. ODP, Sci. Results*, 137/140: College Station, TX (Ocean Drilling Program), 19–34.
- Walker, J.B., and Choppin, G.R., 1967. Thermodynamic parameters of fluoride complexes of the lanthanides. *Adv. Chem.*, 71:127–140.
- Weaver, J.S., and Langmuir, C.H., 1990. Calculation of phase equilibrium in mineral-melt systems. *Comput. Geosci.*, 16:1–19.
- Wood, S.A., 1990. The aqueous geochemistry of the rare-earth elements and yttrium, I. Review of available low-temperature data for inorganic complexes and the inorganic REE speciation of natural waters. *Chem. Geol.*, 82:159–186.
- Zuleger, E., Alt, J.C., and Erzinger, J.A., 1995. Primary and secondary variations in major and trace element geochemistry of the lower sheeted dike complex: Hole 504B, Leg 140. In Erzinger, J., Becker, K., Dick, H.J.B., and Stokking, L.B. (Eds.), *Proc. ODP, Sci. Results*, 137/140: College Station, TX (Ocean Drilling Program), 65–80.

Date of initial receipt: 23 August 1994

Date of acceptance: 29 January 1995

Ms 148SR-114